

Defraeye T., Derome D., Aregawi W., Cantré D., Hartmann S., Lehmann E., Carmeliet J., Voisard F., Verboven P., Nicolai B. (2014), Quantitative neutron imaging of water distribution, venation network and sap flow in leaves, *Planta* 240 (2), 423-436. <http://dx.doi.org/10.1007/s00425-014-2093-3>

<http://dx.doi.org/10.1007/s00425-014-2093-3>**Title:** Quantitative neutron imaging of water distribution, venation network and sap flow in leaves

**Authors:** **Thijs Defraeye**<sup>1,\*</sup> (thijs.defraeye@biw.kuleuven.be), **Dominique Derome**<sup>4</sup> (dominique.derome@empa.ch), **Wondwosen Aregawi**<sup>1</sup> (wondwosenabebe.Aregawi@biw.kuleuven.be), **Dennis Cantré**<sup>1</sup> (dennis.cantre@biw.kuleuven.be), **Stefan Hartmann**<sup>2</sup> (stefan.hartmann@gmx.ch), **Eberhard Lehmann**<sup>2</sup> (eberhard.lehmann@psi.ch), **Jan Carmeliet**<sup>3,4</sup> (jan.carmeliet@empa.ch), **Frédéric Voisard**<sup>5</sup> (frederic.voisard@mail.mcgill.ca), **Pieter Verboven**<sup>1</sup> (pieter.verboven@biw.kuleuven.be), **Bart Nicolai**<sup>1,6</sup> (bart.nicolai@biw.kuleuven.be)

### **Affiliations:**

<sup>1</sup> *MeBioS, Department of Biosystems, University of Leuven, Willem de Croylaan 42, 3001 Heverlee, Belgium*

<sup>2</sup> *Paul Scherrer Institute (PSI), 5234 Villigen, Switzerland*

<sup>3</sup> *Chair of Building Physics, Swiss Federal Institute of Technology Zurich (ETHZ), Wolfgang-Pauli-Strasse 15, 8093 Zürich, Switzerland*

<sup>4</sup> *Laboratory for Building Science and Technology, Swiss Federal Laboratories for Materials Testing and Research (Empa), Überlandstrasse 129, 8600 Dübendorf, Switzerland*

<sup>5</sup> *Department of Materials Engineering, McGill University, M.H. Wong Building, 3610 University Street, Montréal, Québec H3A 0C5, Canada*

<sup>6</sup> *VCBT, Flanders Centre of Postharvest Technology, Willem de Croylaan 42, 3001 Heverlee, Belgium*

### **Main conclusion**

Quantitative neutron imaging is a promising technique to investigate leaf water flow and transpiration in real time and has perspectives towards studies of plant response to environmental conditions and plant water stress

### **Corresponding author:**

Dr. Thijs Defraeye

Division of Mechatronics, Biostatistics and Sensors (MeBioS)

Department of Biosystems (BIOSYST)

KU Leuven

Willem de Croylaan 42, 3001 Heverlee, Belgium

Tel. +32 (0)16 32 16 18 / Fax. +32 (0)16 32 29 66

Defraeye T., Derome D., Aregawi W., Cantré D., Hartmann S., Lehmann E., Carmeliet J., Voisard F., Verboven P., Nicolai B. (2014), Quantitative neutron imaging of water distribution, venation network and sap flow in leaves, *Planta* 240 (2), 423-436. <http://dx.doi.org/10.1007/s00425-014-2093-3>

thijs.defraeye@biw.kuleuven.be

## **Abstract**

The leaf hydraulic architecture is a key determinant of plant sap transport and plant-atmosphere exchange processes. Non-destructive imaging with neutrons shows large potential for unveiling the complex internal features of the venation network and the transport therein. However, it was only used for two-dimensional imaging without addressing flow dynamics, and was still unsuccessful in accurate quantification of the amount of water. Quantitative neutron imaging was used to investigate, for the first time, the water distribution in veins and lamina, the three-dimensional venation architecture and sap flow dynamics in leaves. The latter was visualised using D<sub>2</sub>O as a contrast liquid. A high dynamic resolution was obtained by using cold neutrons and imaging relied on radiography (2D) as well as tomography (3D). The principle of the technique was shown for detached leaves, but can be applied to in-vivo leaves as well. The venation network architecture and the water distribution in the veins and lamina unveiled clear differences between plant species. The leaf water content could be successfully quantified, though still included the contribution of hydrogen in the leaf dry matter. The flow measurements exposed the hierarchical structure of the water transport pathways and accurate quantification of the absolute amount of water uptake in the leaf was possible. Particular advantages of neutron imaging, as compared to X-ray imaging, were identified. Quantitative neutron imaging is a promising technique to investigate leaf water flow and transpiration in real time and has perspectives towards studies of plant response to environmental conditions and plant water stress.

## **Keywords**

neutron imaging, venation, flow dynamics, leaves, tomography, non-destructive

## **INTRODUCTION**

Leaves play a key role in water transport within plants, as the majority of the plant water loss occurs by transpiration via the leaves (Nobel 2005, Jasechko et al. 2013). Leaves are also critical determinants of the earth biosphere, as they are considered the most important moisture sources in the plant canopy (Schuepp 1993). Sap transport in these plant organs and their exchange with the environment is, however, still not fully understood (Sack et al. 2004; Bauerle & Bowden 2011a,b) and is inherently related to the hydraulic architecture of the leaf's sap transport network. The leaf venation system can be considered as a hydraulic network of leaky conduits which has two main functions (Roth-Nebelsick et al. 2001; Zwieniecki et al. 2002), namely mechanical support of the lamina and transport of substances, i.e., of water and solutes to the entire leaf via the xylem, and of water and solutes plus photo-assimilates to other plant organs via the phloem. A large diversity in leaf venation patterns exists between plant species and the relation between the specific venation architecture and the leaf functional properties is not yet fully understood (Roth-Nebelsick et al. 2001). Knowledge of the leaf venation architecture and water distribution in the lamina, as well as of dynamic sap transport in leaves is thus imperative for a better understanding of plant structure-function relationships and plant growth (Brodribb et al. 2007 2010; Kholova et al. 2010) but also plant response to environmental changes (Bauerle et al. 2009; Rogiers et al. 2009). Such knowledge would also contribute to our understanding of leaf transpiration kinetics and plant water stress, the latter being one of the main abiotic factors limiting crop yield (Lambers et al. 2008).

Insight in the leaf hydraulic system and its sap flow dynamics has been obtained using several experimental techniques. The leaf venation structure was often studied destructively (see Pérez-Harguindeguy et al. 2013), but has also been imaged in a non-destructive way with microscopy (Rolland-Lagan et al. 2009; Dhondt et al. 2012) and with X-ray radiography (Wing 1992; Blonder et al. 2012), amongst others. The hydraulic resistance of different components in the venation system has been quantified destructively, to identify the venation hierarchy (Zwieniecki et al. 2002; Sack et al. 2004). Sap flow in leaves has been investigated in real-time with non-destructive techniques such as dye infiltration (Altus & Canny 1985; Jeje 1985) and X-ray radiography (Lee & Kim 2008; Kim & Lee 2010), which allowed determination of flow velocities. Magnetic resonance imaging (MRI) was applied for flow in shoots (Windt et al. 2006; Kaufmann et al. 2009), but this technique also shows perspectives for real-time flow measurements in leaves (van As et al. 2009), as was recently explored (Sardans et al. 2010). The high spatial (700 nm, Verboven et al. 2008; 400 nm, Dhondt et al., 2010; 1660 nm, Blonder et al., 2012) and temporal resolution (exposure time down to 450 ms; Blonder et al., 2012) of (micro) X-ray imaging make it particularly suitable for

Defraeye T., Derome D., Aregawi W., Cantré D., Hartmann S., Lehmann E., Carmeliet J., Voisard F., Verboven P., Nicolai B. (2014), Quantitative neutron imaging of water distribution, venation network and sap flow in leaves, *Planta* 240 (2), 423-436. <http://dx.doi.org/10.1007/s00425-014-2093-3>

studies on a small scale and involving fast phenomena, such as xylem vessel refilling (Kim & Lee, 2010). X-ray imaging however has a relatively low sensitivity and contrast with respect to water. MRI on the other hand provides a higher sensitivity to water, but has a much lower spatial and temporal resolution (~ 30-40  $\mu\text{m}$ , ~ 15-30 min; van As et al. 2009).

A promising alternative to visualise but especially quantify water distribution within leaves (veins and lamina), to identify water transport pathways and thus the hierarchy of the venation network and to investigate real-time water transport within leaves is neutron imaging. Despite its potential, this non-destructive technique however remained virtually unexplored for these purposes, as detailed further below. Although its spatial and temporal resolution are lower (spatial: tens of microns, Anderson et al. 2009; temporal: tens of seconds in the present study) than X-ray imaging (e.g. > 100 nm, Verboven et al. 2008), neutron imaging provides a higher dynamic resolution with respect to water (i.e., the number of grey scales, thus the maximum achievable contrast): the neutron beam is attenuated significantly by the hydrogen in water (Anderson et al. 2009). This implies a strong reduction of the beam intensity when passing through water-containing materials by both neutron scattering and absorption, whereas X-rays are attenuated due to their interaction with the electrons in the atoms, of which water only has a few. As such, neutron imaging is a very suitable technique to visualise and also quantify water in biological tissues, such as plant organs or fruits, since they are predominantly composed of water (e.g., Defraeye et al. 2013): leaves typically contain mostly water (~ 70-95% in mass) but also air (~ 30% in volume) and leaf tissue material (Nobel 2005; Lambers et al. 2008). With neutron imaging, the amount of water in the sample can be quantified almost directly from the radiograms, after some minor corrections, which is often not that straightforward for X-ray imaging and MRI. In particular cold neutrons provide a higher contrast, compared to thermal neutrons, since they have a lower energy level and thereby they induce more beam attenuation (absorption and scattering) within the sample as the attenuation increases with decreasing energy level of the beam. The resulting higher sensitivity for hydrogen is especially beneficial for thin samples such as leaves, which typically have thicknesses of a few hundred  $\mu\text{m}$  (Nobel 2005). Furthermore, cold neutrons also allow the use of thinner scintillators, which enhances spatial resolution.

The use of neutron imaging to study water distribution within leaves, the venation network and real-time water transport within leaves needs to be explored more in detail to evaluate to what extent it could be an alternative non-destructive imaging technique for these purposes, compared to X-ray imaging and MRI. Neutron radiography and tomography have already been used to investigate the

Defraeye T., Derome D., Aregawi W., Cantré D., Hartmann S., Lehmann E., Carmeliet J., Voisard F., Verboven P., Nicolai B. (2014), Quantitative neutron imaging of water distribution, venation network and sap flow in leaves, *Planta* 240 (2), 423-436. <http://dx.doi.org/10.1007/s00425-014-2093-3>

water distribution or transport in plant organs such as roots (Carminati et al. 2010; Esser et al. 2010; Moradi et al. 2011), flower peduncles (Matsushima et al. 2009), seeds (Cleveland et al. 2008) and fruit tissue (Defraeye et al. 2013). Radiography implies that a neutron beam is sent through the plant organ after which its projection is captured by a detector. As a certain amount of the radiation is absorbed and scattered by the material, which is called beam attenuation, contrast appears in the 2D image. A tomography is obtained by taking multiple radiograms at different angles, by rotating the sample, after which this image information is reconstructed to obtain a 3D representation of the object. For leaves, neutron radiography has been applied to estimate changes in leaf water content during dehydration (Matsushima et al. 2005a), to visualise the damage to leaves by vacuum cooling (Kawabata et al. 2005) and to estimate the amount of water in leaves (Matsushima et al. 2005b).

Regarding this previous neutron imaging research on leaves, only neutron radiography was used for leaves, whereas tomography would reveal much more details on the water distribution in both veins and lamina and on the venation architecture. Also, a quantification of the water content in leaves was not yet successful (Matsushima et al. 2005b), mainly due to neutron scattering effects within the sample. By applying appropriate corrections, amongst others for scattering, it was recently shown that accurate quantitative analysis is possible with neutron imaging (Hassanein et al. 2005, not for leaves), with errors in water thickness below 5%. Such a quantification would shed more light on the water distribution within leaves, particularly on differences between veins and lamina. Furthermore, the potential of non-destructive imaging techniques (e.g., X-ray) for the real-time analysis of water transport processes in leaves, by uptake of contrast liquids, has recently been brought up (Blonder et al. 2012), but was only explored for single xylem vessels without contrast agents (Kim & Lee 2010) and not yet for an entire leaf. Neutron imaging is a viable alternative to study real-time water transport in leaves, by using heavy water ( $D_2O$ ) as a contrast liquid tracer, as deuterium attenuates the neutron beam much less than hydrogen.

In this article we evaluate if neutron imaging can successfully be used to image and quantify the water distribution in the lamina and venation network, as well as the flow dynamics in leaves non-destructively and real-time, both in 2D and 3D. For this purpose, quantitative neutron imaging is applied to leaves of apple tree and tomato plant, because they are important tree crops and horticultural crops, respectively. Neutron tomography is used, for the first time, to unveil the water distribution in both types of leaves, in the lamina as well as the venation network, including the leaf

Defraeye T., Derome D., Aregawi W., Cantré D., Hartmann S., Lehmann E., Carmeliet J., Voisard F., Verboven P., Nicolai B. (2014), Quantitative neutron imaging of water distribution, venation network and sap flow in leaves, *Planta* 240 (2), 423-436. <http://dx.doi.org/10.1007/s00425-014-2093-3>

petiole. The accuracy of the leaf water content quantification, from neutron radiograms, is evaluated by comparison with gravimetric measurements. Furthermore, neutron radiography of D<sub>2</sub>O uptake in these leaves is successfully used to study the sap flow dynamics in real-time and to quantify the water loss from the leaf, induced by transpiration. Such dynamic experiments have not been performed to date but open up perspectives towards the study of influence factors of plant water stress and leaf response to environmental changes. Finally, the advantages and limitations of the technique are discussed and compared to X-ray imaging and MRI, and focus points for future research and refinement of the technique are given.

## **MATERIALS AND METHODS**

### **Materials**

Leaves of two kinds of plant species were used, namely apple (*Malus domestica* Borkh., cv. *Ballerina*) and tomato (*Lycopersicon esculentum* Mill., cv. *Grandella*). Plants were transported to the neutron imaging facility and individual leaves were cut from the plants right before the experiments started. This cutting could induce some embolism in the xylem to some extent, which will be avoided in future experiments by cutting under water. The experiments were performed on September 17 - 19 2012. Two types of imaging experiments were performed, namely tomography of a leaf (TOMO) and radiography of liquid uptake by a leaf, by using D<sub>2</sub>O as a tracer (RAD<sub>2</sub>O). D<sub>2</sub>O is a good contrast liquid for neutron imaging, since it attenuates neutrons much less than H<sub>2</sub>O, implying more transmission of the neutron beam, and it can successfully be transported into biological materials (Matsushima et al. 2009). For the tomography experiments, larger leaves were used (ca. 5 cm) than for the radiography experiments (ca. 2.5 cm) since for the latter the field of view was taken smaller to have a higher resolution. Performing a tomography at such high resolution was not feasible due to the much longer acquisition time required.

### **Neutron imaging facility**

The beamline for Imaging with COLD Neutrons (ICON, [www.psi.ch/sinq/icon/](http://www.psi.ch/sinq/icon/)) of the Swiss spallation neutron source (SINQ) at the Paul Scherrer Institute (PSI, Villigen, Switzerland) was used for the experiments. This beamline relies on a cold neutron beam, on which more details can be found in Kaestner et al. (2011a). Fig. 1 shows a schematic overview of the beamline with the test setup. The detector consists of a scintillator-CCD camera system with a total field of view of 96 x 113 mm<sup>2</sup> (for TOMO) and 28 x 28 mm<sup>2</sup> (for RAD<sub>2</sub>O). The scintillator, made of 50 μm (for TOMO) or 20 μm (for RAD<sub>2</sub>O) thick zinc sulfide doped with 6Li as the neutron absorbing agent, converts

Defraeye T., Derome D., Aregawi W., Cantré D., Hartmann S., Lehmann E., Carmeliet J., Voisard F., Verboven P., Nicolai B. (2014), Quantitative neutron imaging of water distribution, venation network and sap flow in leaves, *Planta* 240 (2), 423-436. <http://dx.doi.org/10.1007/s00425-014-2093-3>

the transmitted neutron beam signal into visible light photons. The photons are then led via a mirror onto a cooled 16-bit CCD camera (TOMO: 2160 x 2560 pixels, RAD<sub>2</sub>O: 2048 x 2048 pixels). For the RAD<sub>2</sub>O experiments, two by two binning of the pixels was applied, resulting in 1024 x 1024 binned pixels, since the physical achievable resolution due to focussing and the scintillator was lower (~ 30 μm) than the maximal attainable pixel resolution of the camera (13.5 μm). As such, imaging at this high resolution was unfounded. For tomography, a larger field of view was chosen to limit scanning times to about two hours. The attained spatial (pixel) resolution was 44 μm (TOMO) and 27 μm (RAD<sub>2</sub>O), which is close to the current lower limit for neutron imaging (Anderson et al. 2009). The amount of reactor facilities which produce neutrons is limited. Beamtime can be bought or granted after submitting a project application. In case of the latter, the granted beamtime is typically a few days. Three days were granted in the present study.

### **Neutron experiments**

Two test setups were designed (Supplemental Fig. S1). For the tomography experiments (TOMO), a leaf was mounted between two aluminium plates, which were sealed at the edges with aluminium tape to reduce dehydration during scanning. For the D<sub>2</sub>O uptake experiments (RAD<sub>2</sub>O), a leaf was carefully fixed on an aluminium plate with aluminium tape at its edges (with petiole downwards). The petiole was placed in a small container filled with D<sub>2</sub>O. To enhance the D<sub>2</sub>O uptake thus water loss, the abaxial side, with a higher stomatal density, was exposed to the air and photosynthesis was enhanced by illumination with a small halogen light. The light was at more than a meter distance from the leaf. For the tomato leaf, the light was only switched on one hour after the start of the experiment. To verify the possible toxicity of D<sub>2</sub>O for the plant leaf, we placed a leaf for a prolonged time in both D<sub>2</sub>O and water. The absence of visual differences between both leaves (e.g. no faster wilting) serves as a first indication that the toxicity of D<sub>2</sub>O was limited.

Leaves, including full petioles, were cut from the plant and were mounted on the respective setups (Supplemental Fig. S1). The time interval between removing the leaves from the plant and the first neutron radiogram was about ten minutes, including the time required to securely close the beamline. For the TOMO experiments, three tomato leaves and two apple leaves were scanned, where 226 radiograms were taken (exposure time 20s) over a total range of 180°, which took about two hours for each leaf. For the RAD<sub>2</sub>O experiments, only one leaf of each species was evaluated. No repetitions were performed here due to the long duration of the RAD<sub>2</sub>O experiments and since the beamtime at the neutron facility was limited (three days). Here, a reference neutron radiogram of the leaf was taken after mounting, i.e., at its initial state, and the subsequent radiograms were

acquired at a time interval of less than one minute (exposure time 30s). The RAD<sub>2</sub>O experiment was performed for about five hours for the tomato leaf and eight hours for the apple leaf.

The conditions of the air in the ICON beamline varied to some extent with time but were quite stable over one experiment. For the TOMO experiments, the mean temperature was 25.8°C (standard deviation = 0.6°C) and the mean relative humidity was 40% (standard deviation of 2%). For the RAD<sub>2</sub>O experiments, the mean temperature was 26.2°C (standard deviation of 0.3°C) and the mean relative humidity was 37% (standard deviation = 6%). For the TOMO experiments, the mass of the leaves was measured before mounting (initial mass  $m_0$ , kg), after the measurements ( $m_f$ , kg) and after oven drying the sample (at 60°C) until it was completely dry ( $m_d$ , kg). The mass loss during scanning and the initial mass of water in the leaf ( $m_{w,0}$ , kg) were then determined. The latter was used for comparison with the initial mass of water predicted from the neutron radiograms (see next section below). Gravimetric measurements were not performed for the RAD<sub>2</sub>O experiments, since some leaf tissue stuck to the tape and was lost.

## **Quantification of water in leaves from neutron radiograms**

### Mass of water

The procedure to estimate the amount of water in a leaf from a neutron radiogram is briefly explained. Neutron radiography is based on intensity measurements of a neutron beam transmitted through an object (Fig. 1). The intensity of the transmitted beam ( $I$ ) can be described with the Beer-Lambert law:

$$I = I_0 e^{-\Sigma z} \quad (1)$$

where  $I_0$  is the intensity of the incident neutron beam,  $z$  is the thickness of the object along the beam direction (m) and  $\Sigma$  is the effective attenuation coefficient for neutrons ( $\text{m}^{-1}$ ). For a compound material like leaf tissue or water, the attenuation coefficients of the individual elements (mainly hydrogen, but also oxygen, carbon, etc.) determine the total beam attenuation (scattering and absorption). The composition of the leaves was simplified by assuming them to consist at each point (pixel in the radiograms) of leaf dry matter and water, using a bi-layer approximation (see Sedighi-Gilani et al. 2012). Thus, the effect of the water present in the leaf tissue on the neutron beam attenuation was considered equivalent to the effect of a water layer with thickness  $z_w$  (m)

added to the leaf dry matter. In addition, the neutron beam was also attenuated by the aluminium test setup (Supplemental Fig. S1). Implementing this in Eq. (1) results in:

$$I = I_0 e^{-(\Sigma_{TS} z_{TS} + \Sigma_{LT} z_{LT} + \Sigma_w z_w)} \quad (2)$$

where the subscript *TS* refers to the test setup, *LT* to the dry matter of the leaf tissue and *w* to the water (liquid and vapour). Eq. (2) can in principle be solved to the water thickness ( $z_w$ ), i.e., the amount of water (in meters) in each pixel of a radiogram of the leaf, by subtracting the influence of the test setup and the leaf dry matter. The attenuation coefficient of the leaf dry matter ( $\Sigma_{LT}$ ) was, however, difficult to determine due to its complex composition; also, scattering corrections of the neutron radiograms, for leaf dry matter in particular (see below), could not be made. Furthermore, the exact leaf thickness ( $z_{LT}$ ) was also unknown. As such, the beam attenuation by the hydrogen present in the leaf (but also by other attenuating elements), could not be quantified, by which  $z_w$  could not be determined at the time being. Instead, an effective water thickness of the leaf ( $z_{w,eff}$ ) was determined, in which the influence of the leaf dry matter was inherently included.  $z_{w,eff}$  is defined as follows, and can be rewritten using Eq. (2):

$$z_{w,eff} = z_w + \frac{\Sigma_{LT}}{\Sigma_w} z_{LT} = -\frac{1}{\Sigma_w} \left[ \ln \left( \frac{I}{I_0} \right) + \Sigma_{TS} z_{TS} \right] \quad (3)$$

This water thickness in the radiograms is the resulting value per pixel in the image. Although the influence of leaf dry matter on beam attenuation was expected to be limited, as water is the main constituent of a leaf, the hydrogen present in the leaf tissue (but also other attenuating elements) did interact to some extent with the neutron beam, as discussed below in detail. This effective thickness thus contains a contribution for the leaf tissue in each individual pixel. This leaf-tissue contribution will vary spatially over the leaf, as veins contain more tissue than the leaf lamina, for example. However, since this leaf-tissue contribution to  $z_{w,eff}$  at a certain position (pixel) is constant, i.e. it does not vary with water content in the leaf, the observed changes in  $z_{w,eff}$  are representative for changes in the amount of water within the leaf. If excessive shrinkage or swelling during dehydration or rehydration would occur however, this does not hold anymore. In the present study, shrinkage was very limited though. Recent studies on leaf shrinkage are Blonder et al. (2012) and

Defraeye T., Derome D., Aregawi W., Cantré D., Hartmann S., Lehmann E., Carmeliet J., Voisard F., Verboven P., Nicolai B. (2014), Quantitative neutron imaging of water distribution, venation network and sap flow in leaves, *Planta* 240 (2), 423-436. <http://dx.doi.org/10.1007/s00425-014-2093-3>

Scoffoni et al. (2013). From this effective water thickness, the effective water mass thickness ( $Z_{w,eff}$ ,  $\text{kg m}^{-2}$ ) was determined for every pixel in the radiogram:

$$Z_{w,eff} = \rho_w z_{w,eff} \quad (4)$$

where  $\rho_w$  is the density of water ( $\text{kg m}^{-3}$ ). The total mass of water in the leaf ( $m_{w,eff,tot}$ , kg) was then calculated as:

$$m_{w,eff,tot} = Z_{w,eff,avg} A_f \quad (5)$$

where  $A_f$  is the frontal area of the sample as seen in the radiogram ( $\text{m}^2$ ), which was determined manually, and  $Z_{w,eff,avg}$  is the surface-averaged value (over all pixels) of the water mass thickness ( $Z_{w,eff}$ ) within  $A_f$ . Eqs. (3)-(4) allowed calculation of the spatial distribution of the water (mass) thickness. The influence of the test setup in Eq. (3) was accounted for by determining an average value of the water thickness of the aluminium setup in an area outside the sample from the radiograms and by subtracting this average value from all pixels.

#### Water loss during $D_2O$ uptake

For the  $\text{RAD}_2\text{O}$  experiments, the beam attenuation in the leaf sample changed over time, with respect to the initial state, due to  $D_2O$  uptake into the leaf xylem and water loss via transpiration. Secondary effects include water flow out of the leaf via the phloem into the  $D_2O$  container and the conversion of water into photo-assimilates by photosynthesis, which are both considered limited. As such, these secondary effects did not change the overall beam attenuation significantly. The  $D_2O$  uptake and water loss both caused a reduction of the effective water thickness ( $z_{w,eff}$ ) over time ( $t$ ). This reduction in water thickness ( $\Delta z_w(t) < 0$ ) could be quantified as follows (see Supplemental Notes S1):

$$\Delta z_w(t) = -\frac{1}{(\Sigma_w - \Sigma_{D_2O})} \left[ \ln \left( \frac{I(t)}{I(t_0)} \right) \right] \quad (6)$$

where  $I(t_0)$  is the intensity of the neutron beam for the initial, freshly-cut leaf sample, i.e., at the start of the neutron experiments ( $t_0$ ), and the subscript  $D_2O$  refers to heavy water. Note that,

Defraeye T., Derome D., Aregawi W., Cantré D., Hartmann S., Lehmann E., Carmeliet J., Voisard F., Verboven P., Nicolai B. (2014), Quantitative neutron imaging of water distribution, venation network and sap flow in leaves, *Planta* 240 (2), 423-436. <http://dx.doi.org/10.1007/s00425-014-2093-3>

although neutrons attenuate much stronger for water than for D<sub>2</sub>O ( $\Sigma_{D_2O} = 0.5 \text{ cm}^{-1}$ ,  $\Sigma_w = 5.13 \text{ cm}^{-1}$  in the present study, see Supplemental Notes S1), neutron imaging is still sufficiently sensitive to distinguish changes in D<sub>2</sub>O as well. Note that this reduction in water thickness is not affected by a leaf-tissue contribution, as the latter is constant over time at a certain location and thereby vanishes from  $\Delta z_w(t)$ .

Similar to Eqs. (4)-(5), the change in water mass thickness ( $\Delta Z_w(t) < 0$ ) and the total water loss of the sample over time ( $\Delta m_{w,tot}(t) < 0$ ) were determined as:

$$\Delta Z_w(t) = \rho_w \Delta z_w(t) \quad (7)$$

$$\Delta m_{w,tot}(t) = \Delta Z_{w,avg}(t) A_f \quad (8)$$

where  $\Delta Z_{w,avg}(t)$  is the surface-averaged value (over all pixels) of  $\Delta Z_w$  within  $A_f$ .

### Image correction and tomographic reconstruction

Prior to quantitative analysis (e.g., from Eq. (3)), each raw neutron radiogram was corrected. These corrections use standard procedures common to all radiation transmission-based imaging methods, together with a neutron scattering correction as required for neutron radiography, which are detailed in Supplemental Notes S2.

For the TOMO experiments, a tomogram was reconstructed from the individual radiograms, by means of the Octopus software (UGCT, Ghent, Belgium). Since there was some water loss during the tomograms (see Results section), no image correction towards quantification was performed (see Supplemental Notes S2) for tomographic reconstructions and only flat field and dark current corrections were made.

A water thickness resolution of 0.1  $\mu\text{m}$  (TOMO) and 0.14  $\mu\text{m}$  (RAD<sub>2</sub>O) was obtained, which resulted in a dynamic range of about 2000 (TOMO) or 700 (RAD<sub>2</sub>O) greyscale levels detectable over a leaf, assuming a leaf water thickness of 200  $\mu\text{m}$  (TOMO) and 100  $\mu\text{m}$  (RAD<sub>2</sub>O).

Corresponding resolutions for water content are 0.5  $\text{kg m}^{-3}$  and 1.4  $\text{kg m}^{-3}$ .

## **RESULTS**

### **Quantitative neutron imaging**

The total mass of water in the leaf as determined from neutron imaging ( $m_{w,eff,tot}$ ) cannot not exactly represent the actual mass of water in the leaf, as the hydrogen (but also other attenuating elements) present in the leaf dry matter was inherently included (Eq.(3)). In order to quantify the contribution of the leaf dry matter on the neutron beam attenuation and, hence, to assess the accuracy of the water quantification, we wanted to compare the neutron-calculated water mass with the water mass that was determined gravimetrically ( $m_{w,0}$ ). For this purpose, the water mass calculated from the first neutron radiogram at the start of each TOMO experiment was used ( $m_{w,eff,tot}$ , Eq. (5), see Materials and Methods).

In Table 1, the water mass inside the leaves ( $m_{w,0}$ ), the percentage mass of the leaf dry matter ( $m_d/m_{w,0}$ ) and the average water thickness ( $z_{w,0,avg} = m_{w,0}/(A_f \rho_w)$ , m) are given, as determined from the gravimetric measurements. The water mass as obtained from the initial neutron radiograms is also shown and the percentage difference in mass between the two methods is given, as well as the leaf surface area. This difference is defined as  $(m_{w,eff,tot} - m_{w,0})/m_{w,0}$ , thus positive percentages imply that more water is found in the neutron radiograms. Similar data are also given for the water mass, when a sample scattering correction (see Supplemental Notes S2 and Hassanein et al. (2005)) is not accounted for in the neutron radiograms ( $m_{w,eff,tot,ns}$ ). A scattering correction is usually required since many materials attenuate the neutron beam by scattering rather than absorption. Since these scattered neutrons can still reach the detector, they increase the intensity of the images (as there is more transmission), which can then be interpreted erroneously as a lower water thickness in the sample (Hassanein et al. 2005). Hence a scattering correction is applied to resolve this unwanted side-effect and to obtain a more realistic (higher) water thickness.

The average water thickness varies between 140 and 230  $\mu\text{m}$ . These values are typical for leaves, as they have a thickness of a few hundred  $\mu\text{m}$  and are mainly composed out of water (Nobel 2005). The differences between gravimetric and neutron imaging (with scattering) methods are much larger for apple leaves ( $\sim 30\%$ ) than for tomato leaves ( $\sim 5\%$ ). This is mainly attributed to the higher percentage of dry matter in the apple leaf ( $\sim 35\%$ ) compared to the tomato leaf ( $\sim 10\%$ ): as the leaf dry matter also contains hydrogen, it contributes to the effective water thickness ( $z_{w,eff}$ ), leading to a higher predicted water mass in the neutron radiograms ( $m_{w,eff,tot}$ ). The leaf dry matter

Defraeye T., Derome D., Aregawi W., Cantré D., Hartmann S., Lehmann E., Carmeliet J., Voisard F., Verboven P., Nicolai B. (2014), Quantitative neutron imaging of water distribution, venation network and sap flow in leaves, *Planta* 240 (2), 423-436. <http://dx.doi.org/10.1007/s00425-014-2093-3>

thus accounts for a significant amount of neutron attenuation, leading to a higher apparent water thickness in the radiograms, and cannot be neglected for some species, as evident here for apple leaves, by the large differences observed. As such, future steps towards corrections for the leaf tissue contribution are essential here, as discussed below more in detail. Note however that for some samples (tomato leaves in this study), the impact of the leaf dry matter is very limited.

Without a scattering correction (Table 1), the water mass seems to agree better with the gravimetric measurements (~ 1% for tomato and ~ 20% for apple). However, a negative value is found for tomato which is in principle impossible since the neutron radiograms should always predict a higher apparent water mass due to the hydrogen in the leaf dry matter. Therefore, a scattering correction seems necessary here, even for very small water thicknesses such as those found in a leaf, but this correction has a limited influence, as differences in the water mass due to such corrections are about 6% for both apple and tomato leaves.

### **Leaf water distribution and venation architecture**

Next, we wanted to unveil the hydraulic architecture of the leaves by visualising the water distribution within the lamina and veins from both single neutron radiograms as well as reconstructed tomograms. With respect to the radiograms, only the initial radiogram was taken to calculate the effective water thickness distribution ( $z_{w,eff}$ ), due to the D<sub>2</sub>O uptake in the RAD<sub>2</sub>O experiments and since the leaf water mass decreased to some extent during the TOMO experiments. The latter was caused by water transpiration, even though the leaf was between plates which were sealed with tape. This mass loss was between 3% and 9%, depending on the sample. These effective water thickness distributions across the leaf surface from the radiograms of TOMO and RAD<sub>2</sub>O experiments are shown in Fig. 2 and Fig. 3 respectively, and are scaled with the average effective water thickness over the entire leaf ( $z_{w,eff,avg}$ ). The RAD<sub>2</sub>O experiments involved smaller leaves at a higher spatial resolution.

The differences in water distribution and venation architecture between tomato and apple leaves can clearly be distinguished from the neutron radiograms (Figs. 2-3). Particularly the first and second order veins are visible in the TOMO radiograms. The RAD<sub>2</sub>O radiograms additionally unveil venation architecture at a lower hierarchical level (see focus in Fig. 3): for apple leaves, a fine network of third order veins is apparent; for tomato leaves, the water outside the first and second order veins is rather homogeneously distributed within the mesophyll tissue of the leaf lamina instead of in low-level venation. A higher resolution (RAD<sub>2</sub>O vs. TOMO) thus allowed

identification of a lower hierarchical level of venation. Note that the water thickness shown for the vascular system inherently includes both free water in the veins and cellular water within the cells of the vascular tissue. In addition, it has to be kept in mind that the presented effective water thickness distributions in Figs. 2-3 inherently include a leaf-tissue contribution, which varies spatially over the leaf. Since the veins do not only contain most of the water, due to their larger thickness, but also a bit more leaf tissue than the leaf lamina, the reported effective water thicknesses for the veins are expected to differ somewhat more from the actual water thickness than for the leaf lamina, i.e. they will be slightly higher. Though a quantification of the leaf-tissue contribution was not feasible in the present study, this is a critical focus point for future enhancement of neutron imaging of leaves or other biological tissues.

Tomograms of two leaves are shown in Supplemental Fig. S2, in which the first and second order veins of the 3D venation architecture are highlighted. Lower venation levels were more difficult to segment (i.e., distinguishing different tissues from 3D imaging, based on contrast differences) as their water content was very similar to that of the leaf lamina. The venation architecture is more sharply defined in the tomograms than in a single radiogram, which has a more blurry appearance, since information from multiple radiograms is combined in a tomogram, but is still not optimal due to some shrinkage involved during the tomography (see Discussion section). As the resolution of neutron imaging techniques is continuously increasing, we expect that lower venation levels will become more clearly visible with neutron imaging in the coming decade. With respect to quantification however, the results from tomography are less reliable due to the aforementioned mass loss during scanning, which is inherently incorporated in the reconstructed tomograms. Due to this unavoidable error, a quantification of the amount of water in the leaves from tomograms was not pursued in this study. Nevertheless, the (relative) internal water content distribution inside the leaf ( $w$ , determined per voxel of the 3D tomogram,  $\text{kg m}^{-3}$ ) could be extracted from the tomograms by scaling with the maximal value ( $w_{max}$ ) in each image. It is shown in Fig. 4 for a section through the petioles of each of the leaves and in Fig. 5 for various sections through two leaves, where each section is scaled separately with its  $w_{max}$ . In these figures, the water content per (3D) voxel is represented. Although a distinct gradient in water content can be seen near the surface of the petiole (Fig. 4), i.e., over the epidermis and collenchyma tissue, individual tissue types in the petiole (xylem, phloem, parenchyma, etc.) cannot be distinguished so the resolution of neutron imaging is too limited for this purpose, at the used size of petioles. The veins clearly stand out in the cross sections (Fig. 5). Note however that also here, the leaf dry matter will contribute to the reported amount of water in the leaf, particularly in the veins and petioles, which can affect the observed

water distribution to some extent. The water distribution in the lamina of the apple leaf is more heterogeneous than in the tomato leaf, due to the fine network of veins, which is particularly pronounced in the upper part of the leaf.

### **Water transport in leaves**

In order to quantify the water transport through the vascular system, we carried out an experiment (RAD<sub>2</sub>O) in which D<sub>2</sub>O was taken up by the vascular system via the xylem, replenishing it for the water losses resulting from transpiration, and secondary (minor) losses due to photosynthesis and water flow out of the leaf back into the container via the phloem. The progression of D<sub>2</sub>O into the vascular system could be monitored in the radiograms due to its difference in neutron beam attenuation with water. In Table 2, the water mass from the initial neutron radiograms ( $m_{w,eff,tot}$ ), the initial average water thickness ( $z_{w,eff,avg}$ ) and the surface area of the leaves ( $A_f$ ) are given. The D<sub>2</sub>O uptake into the leaf over time is visualised in Fig. 6, by showing the change in water thickness  $\Delta z_w(t)$  (Eq. (6), in absolute value thus  $> 0$ ). This value is scaled with the initial average water thickness of the leaf ( $z_{w,eff,avg}$ ), thus indicating the relative amount of D<sub>2</sub>O uptake/water loss of the leaf. In principle, the observed changes in water thickness do not necessarily imply replacement of water by D<sub>2</sub>O in these regions, but may only indicate the removal of water (e.g., from transpiration), which also would change contrast. However, given the logical pattern of contrast changes, i.e., from the petiole upwards and following the venation network, as well as the fact that the water thickness in the part of the leaf where D<sub>2</sub>O did not protrude initially (e.g., upper part of leaf) remained quasi constant (Fig. 6) are a good indication that the contrast changes were attributed to D<sub>2</sub>O uptake rather than water loss due to transpiration. The fact that the leaf did not look wilted at the end of the experiment also serves as a more qualitative indication that contrast changes were not due to transpiration loss. The quasi constant water thickness in areas not affected (initially) by D<sub>2</sub>O indicates the leaf water status remains about the same: the water loss due to transpiration is replenished locally by supply of water via the vascular system, which in its turn drives D<sub>2</sub>O uptake.

The transport pathways and their hierarchy can be distinguished. With the tomato leaf, transport seems to occur from the first and second order veins directly into the mesophyll tissue, whereas for the apple leaf also transport via the third order veins can be seen. Furthermore, Fig. 6 can be compared with the initial water thickness distribution (Fig. 3), as both have the same scaling. When focussing on the first and second order veins, the lower values in Fig. 6 indicate that even at the end of the uptake experiment, not all water which was initially present, was replaced by D<sub>2</sub>O. This has two reasons: (1) the intracellular water in the petiole (parenchyma, epidermis, etc.) was less easily

replaced by D<sub>2</sub>O than that in the vascular system and even some (free) water might still have been present in the veins (xylem and phloem) at the end of the experiment; (2) the hydrogen in the leaf dry matter (but also other attenuating elements) also contributes to the beam attenuation and cannot be replaced by D<sub>2</sub>O.

The total water mass loss from both leaves ( $\Delta m_{w,tot}$ , Eq. (8), in absolute value thus  $> 0$ ), is shown in Fig. 7. The time when the halogen light was switched on for the tomato leaf is indicated with the dotted line; for the apple leaf, the light was switched on during the entire experiment. Note that the neutron beam went offline for about 20 minutes right after switching on the light for the tomato leaf, but this should not have an effect on the physical processes, so it only implies that no data were available during this period. Slight fluctuations in the mass loss curves appear, where also negative mass losses can be observed, which is in principle impossible. These fluctuations may be attributed to changes in neutron beam intensity which, despite the performed intensity correction (see Supplemental Notes S2), were still manifested in the mass loss curves, though quite limited. As such, the accuracy of the detection method is certainly not higher than about 0.2 mg. Large fluctuations were found, however, for the tomato leaf between 1h and 1.5h, due to significant beam intensity fluctuations, and were removed manually. Apart from beam intensity fluctuations, temporal fluctuations in image intensity could also have been induced by changes in the scattering of the test setup, caused by the changing level of D<sub>2</sub>O in the container during the experiment due to evaporation and refilling.

The tomato leaf shows a response to the light, i.e., by an increased uptake; but with a delay of about half an hour, which is approximately the time scale for stomatal response (~ ten minutes; Mott & Buckley 2000; Nobel 2005; Marengo et al. 2006). This experiment indicates that neutron imaging can successfully be used to investigate the impact of environmental changes (irradiation in this case) on the leaf water transport in real time, which is of particular interest for studies on plant water stress. Furthermore, the water loss by apple and tomato leaves is initially very similar, even though the tomato leaf was not illuminated at that time. This indicates that they have a different transpiration rate under similar environmental conditions. Both water loss profiles are clearly nonlinear. The total leaf water loss, compared to the initial mass of water inside the leaf was 50% for the tomato leaf and 60% for the apple leaf, which had a lower initial water mass and water thickness (Table 2).

## **DISCUSSION**

### **Quantitative neutron imaging**

Compared to previous research on neutron imaging of leaves, an important step was taken towards quantification of the amount of water in leaves in this study. Previous studies looked at differences in amount of water with respect to the initial state during dehydration (Matsushima et al. 2005a) or estimated the amount of water in leaves (Matsushima et al. 2005b). The latter were unsuccessful in quantifying the amount of water, which was attributed to neutron scattering effects within the sample. Although the absolute water mass could not be quantified in the present study due to the presence of hydrogen in the leaf dry matter (but also of other attenuating elements), the effective water mass (of water and leaf dry matter) was successfully quantified from the neutron radiograms. It was shown that the leaf dry matter also contributed to some extent to neutron attenuation (up to 30%), in addition to the water present in the leaf, and thus cannot be neglected. In addition, this leaf-tissue contribution varies spatially over the leaf and will differ for veins and leaf lamina. Hence future research efforts should be directed towards explicitly quantifying the contribution of the leaf dry matter, which requires imaging dried leaf samples. As such, the neutron radiograms could be corrected for it or calibrated a-posteriori, thus revealing only the water present in the leaf. However, for dynamic experiments of water uptake in leaves (e.g., as RAD<sub>2</sub>O) but also leaf dehydration, differences in water content with respect to the initial state are particularly of interest. Hence, the contribution of the leaf tissue disappears when quantifying water thickness differences (Eqs. (6)-(8)). For such dynamic experiments, an absolute and accurate quantification of the change in amount of water can be done with neutron imaging (Fig. 7), which was not reported to date.

Furthermore, a scattering correction is normally not required for low water thicknesses (< 1 mm) when using thermal neutrons, according to Hassanein et al. (2005), and could even result in overestimations up to 30% for thicknesses below 1 mm. In the present experiment with cold neutrons, applying a scattering correction enhanced the accuracy of quantitative neutron imaging, even for thin samples such as leaves, where scattering is limited. The impact of the scattering correction was, however, small (~ 6%).

### **Spatial, temporal and dynamic resolution in relation to other non-destructive techniques**

Apart from such quantification, neutron imaging allowed a direct estimation of the (relative) 3D water distribution within leaves, both in veins and lamina, as well as the water transport pathways

Defraeye T., Derome D., Aregawi W., Cantré D., Hartmann S., Lehmann E., Carmeliet J., Voisard F., Verboven P., Nicolai B. (2014), Quantitative neutron imaging of water distribution, venation network and sap flow in leaves, *Planta* 240 (2), 423-436. <http://dx.doi.org/10.1007/s00425-014-2093-3>

and thus the hierarchy of the venation network. As mentioned, other non-destructive techniques can be applied as well for these purposes, which differ with respect to their spatial, temporal and dynamic resolution. The spatial resolution of neutron imaging is lower (44  $\mu\text{m}$  for TOMO in this study and typically tens of microns for high-resolution neutron imaging; Anderson et al. 2009) than that obtainable by micro X-ray CT (700 nm, Verboven et al. 2008; 400 nm, Dhondt et al., 2010; 1660 nm, Blonder et al., 2012) but is comparable to that of MRI ( $\sim$  30-40  $\mu\text{m}$ , van As et al. 2009). This low resolution does not allow clear distinction of water content gradients over the thickness of the leaf lamina (a few 100  $\mu\text{m}$ ), but only in the first and second order veins (Figs. 5-6). X-ray imaging, potentially in combination with a contrast agent (Blonder et al., 2012), would be more suitable for studies on a smaller scale, amongst others xylem vessel refilling (Kim & Lee, 2010) or water transport at cellular level. The temporal resolution of X-ray imaging (exposure time down to 450 ms; Blonder et al., 2012) is also higher than that of standard neutron imaging (20-30 s for a radiogram in this study), but techniques for faster neutron imaging can be used for particular applications (Anderson et al. 2009). A particular disadvantage of X-ray imaging is that it can damage the tissue (Blonder et al., 2012), which can become problematic in some cases, for example when performing a tomography at high beam intensities (e.g. in a synchrotron). Neutron imaging and MRI do not have this problem.

The dynamic resolution of neutron imaging, i.e., the sensitivity to water, is very high, which is beneficial, amongst others, for segmentation of the tomographic images with respect to the venation architecture. As such, no contrast agents are required, whereas Blonder et al. (2012) had to rely on impregnation with an iodine contrast agent to visualise the vascular network in dried leaves with X-ray imaging. The main strength of neutron imaging, compared to other non-destructive techniques, is that it allows to directly quantify the mass of water and its spatial distribution over the leaf, i.e., with limited corrections or calibration, which is particularly interesting to determine spatial variations and changes in the amount of water in the leaf in real time, as detailed more in the next section.

On the other hand, since the time available for scanning is often limited in reactor facilities which produce neutrons, new experimental setups should be devised which allow scanning several samples together, in order to increase the dataset and to allow more repetitions. This could be done for example by sequential scanning of samples mounted on the same test rig, e.g. by translation of the test rig to bring each sample in succession into the beam. Finally, the limits with respect to

Defraeye T., Derome D., Aregawi W., Cantré D., Hartmann S., Lehmann E., Carmeliet J., Voisard F., Verboven P., Nicolai B. (2014), Quantitative neutron imaging of water distribution, venation network and sap flow in leaves, *Planta* 240 (2), 423-436. <http://dx.doi.org/10.1007/s00425-014-2093-3>

spatial, temporal and dynamic resolution of neutron imaging are continuously improved by technological innovations (Anderson et al. 2009). Nevertheless, these resolution improvements are rather incremental than revolutionary, by which the current limitations of using neutron imaging for studying water transport in leaves will probably still hold for the coming decade.

### **Dynamic monitoring of leaf-environment interactions**

The present experiment indicated that neutron imaging is an appropriate technique to investigate dynamic leaf transport processes in real time in a quantitative way, such as leaf transpiration as well as the impact of environmental changes (e.g., solar radiation) on leaf water transport, which is particularly of interest to study the relation between plant water stress and environmental conditions.

Such dynamic experiments, as liquid uptake in leaves, could be performed with X-rays as well, by using water with a contrast agent to visualise flow, as mentioned by Blonder et al. (2012). A particular difference between the contrast agents for neutrons and X-rays is that D<sub>2</sub>O induces less beam attenuation compared to water, while X-ray contrast agents increase beam attenuation. X-ray contrast agents thus have an opposite effect on beam attenuation, compared to leaf water loss due to transpiration. Despite its higher spatial and temporal resolution, compared to neutron imaging, X-ray imaging has some disadvantages for such liquid uptake experiments: (1) The dynamic resolution (i.e., sensitivity) for water is less than with neutrons. This is particularly important when quantifying pure transpiration (water loss) in the leaf lamina, e.g. on in vivo leaves without the use of contrast agents; (2) Explicit quantification of the amount of liquid (contrast agent) taken up by the leaf as well as the amount of water transpired to the environment remains currently difficult, due to lower sensitivity of X-rays to water (dynamic resolution) and the specific concentration in which the contrast agent is applied; (3) Dedicated software tools which allow direct quantification of the amount of water (change), based on radiograms and attenuation coefficients of the materials and contrast agents (e.g., QNI software for neutrons, Supplemental Notes S2) are not yet available for X-rays to the knowledge of the authors; (4) Each of the many possible X-ray contrast agents available will have a different impact on the leaf water status, which is often unknown and should be assessed, whereas for neutrons, only D<sub>2</sub>O is a widely used contrast agent; (5) some X-ray contrast agents are not very strong, compared to D<sub>2</sub>O for neutron imaging. Note that some of these disadvantages will become particularly pronounced for very thin samples such as leaves. MRI also

Defraeye T., Derome D., Aregawi W., Cantré D., Hartmann S., Lehmann E., Carmeliet J., Voisard F., Verboven P., Nicolai B. (2014), Quantitative neutron imaging of water distribution, venation network and sap flow in leaves, *Planta* 240 (2), 423-436. <http://dx.doi.org/10.1007/s00425-014-2093-3>

shows potential here (van As et al. 2009), and the amount of water can also be determined from the images, but has only recently been explored to monitor transport in leaves (Sardans et al. 2010), where the plant response to stress conditions was successfully monitored (Sardans et al. 2010). Furthermore, next to water, also water mobility can be measured here ( $T_2$  values), which is a unique feature of MRI.

In the present study, the principle of neutron imaging was shown using detached leaves. The main reason was that we wanted to image transport in the vascular network by means of a ( $D_2O$ ) tracer. When only the leaf water status is of interest, e.g., its response under stress conditions or the dehydration of leaves, the leaves can obviously be scanned as well attached to a (small) plant, both using radiography and tomography. Particularly for experiments on the leaf water status of in-vivo (attached) leaves, X-ray imaging is not considered a viable alternative due to its low dynamic resolution for water, but MRI could be applied here. With respect to studying water uptake on in-vivo plants,  $D_2O$  could be introduced via the root system in the plant. The feasibility of this method should be verified first to verify if  $D_2O$  can be successfully introduced in the plant system. X-ray imaging on the other hand, would require that water with a contrast agent is used.

A future challenge when using any imaging technique for analysis of vascular transport will be to distinguish the water transport into the xylem, driven by leaf transpiration, from the sap transport out of the leaf via the phloem. However, directional information will be less straightforward to obtain in any case.

### **Tomography for 3D venation architecture**

Two-dimensional imaging, amongst others by neutron radiograms, already provides detailed information on leaf venation (Dhondt et al. 2012), as a leaf is in most cases a thin 2D ramifying structure without overlap (Roth-Nebelsick et al. 2001), though also 3D venation patterns were unveiled (Ogburn & Edwards 2013). Nevertheless, tomograms have the particular advantage that they characterise the venation architecture in 3D (see Supplemental Fig. S2) and that they can identify the 3D water distribution inside the veins (Figs. 5-6). Such a 3D representation opens up perspectives towards the construction of 3D geometrical models of the actual venation architecture, which could be used for numerical modelling of sap flow through leaves. In the past, 3D (micro)structures of plant organs have been obtained with such 3D imaging techniques (e.g., Kuroki et al. 2004; Mendoza et al. 2007; Verboven et al. 2008; Kaiser 2009; Dhondt et al. 2010; Herremans

Defraeye T., Derome D., Aregawi W., Cantré D., Hartmann S., Lehmann E., Carmeliet J., Voisard F., Verboven P., Nicolai B. (2014), Quantitative neutron imaging of water distribution, venation network and sap flow in leaves, *Planta* 240 (2), 423-436. <http://dx.doi.org/10.1007/s00425-014-2093-3>

et al. 2013) and have been used for numerical modelling purposes of transport processes in these organs (Ho et al. 2011, 2012; Verboven et al. 2012).

As the mass loss (for TOMO) was inherently accompanied by a slight shrinkage of the leaf, the tomograms are less sharp than they would be for a rigid sample and quantification of the amount of water in the tomograms was impeded. The impact of shrinkage, resulting from mass loss, on the quality of the tomogram and on the accuracy of the quantification of the amount of water could perhaps be reduced by acquiring tomograms (of detached leaves) based on non-sequential decompositions of the sample rotation angle sequence (Kaestner et al. 2011b), which was originally developed for 4D imaging. With this fundamentally different tomographic imaging technique, images are not acquired by sequentially rotating the sample over 180°, for example. Instead, images are taken at non-sequential angles over the entire angular range (e.g., 180°), by taking much larger angular steps. As such, a smaller dataset, e.g. the first 50 radiograms, can already be used to successfully reconstruct a tomogram. The faster acquisition of such tomograms, e.g. only 50 images, implies less water loss thus less shrinkage. Of course, evaluating a smaller number of images (e.g. 50) will imply a loss in quality of the tomography, so a trade-off between shrinkage and the amount of images taken will be present. Another option would be to scan a leaf in vivo, as attached to a (small) plant. This procedure is less straightforward for many plants due to space limitations in the beamline.

## **Outlook**

Neutron imaging was shown to be successful in accurately quantifying the absolute amount of transpiration-driven water uptake in a leaf in real time and spatially-resolved, and thus also the pathways via which such water transport takes place. As such, the quantitative neutron imaging technique is currently already applicable for studies on plant responses to environmental conditions and plant water stress. The current spatial and temporal resolution make that the region of interest of this technique will be typically (small) leaves, with a focus on first and second order veins. A critical future improvement of the technique should be to quantify the contribution of the leaf dry matter to the beam attenuation, which would allow to accurately quantify as well the amount of water in a leaf from a single radiography and its corresponding spatial variation.

Defraeye T., Derome D., Aregawi W., Cantré D., Hartmann S., Lehmann E., Carmeliet J., Voisard F., Verboven P., Nicolai B. (2014), Quantitative neutron imaging of water distribution, venation network and sap flow in leaves, *Planta* 240 (2), 423-436. <http://dx.doi.org/10.1007/s00425-014-2093-3>

## **ACKNOWLEDGEMENTS**

This work was supported by the European Commission under the 7th Framework Programme through the 'Research Infrastructures' action of the 'Capacities' Programme, NMI3-II Grant number 283883. Thijs Defraeye is a postdoctoral fellow of the Research Foundation – Flanders (FWO) and acknowledges its support. Financial support by the Research Foundation – Flanders (project FWO G.0645.13) and KU Leuven (project OT 12/055) is also gratefully acknowledged. The experiments were carried out at the ICON beamline (SINQ: Swiss Spallation Neutron Source) of the Paul Scherrer Institute, Villigen, Switzerland. We would like to acknowledge the contributions and support of the Paul Scherrer Institute ICON support team.

## **LITERATURE CITED**

- Altus DP, Canny MJ (1985) Water pathways in wheat leaves. I. The division of fluxes between different vein types. *Aust J Plant Physiol* 12: 173-181.
- Anderson IS, McGreevy R, Bilheux HZ, eds. (2009) *Neutron imaging and applications - A reference for the imaging community*. Springer Science + Business Media, New York.
- Bauerle WL, Bowden JD (2011a) Separating foliar physiology from morphology reveals the relative roles of vertically structured transpiration factors within red maple crowns and limitations of larger scale models. *J Exp Bot* 62: 4295-4307.
- Bauerle WL, Bowden JD (2011b) Predicting transpiration response to climate change: insights on physiological and morphological interactions that modulate water exchange from leaves to canopies. *Hortsci* 46: 163-166.
- Bauerle WL, Bowden JD, Wang GG, Shahba MA (2009) Exploring the importance of within-canopy spatial temperature variation on transpiration predictions. *J Exp Bot* 60: 3665-3676.
- Blonder B, Buzzard V, Simova I, Sloat L, Boyle B, Lipson R, Aguilar-Beaucage B, Andrade A, Barber B, Barnes C, Bushey D, Cartagena P, Chaney M, Contreras K, Cox M, Cueto M, Curtis C, Fisher M, Furst L, Gallegos J, Hall R, Hauschild A, Jerez A, Jones N, Klucas A, Kono A, Lamb M, Matthai JD, McIntyre C, McKenna J, Mosier N, Navabi M, Ochoa A, Pace L, Plassmann R, Richter R, Russakoff B, Aubyn HS, Stagg R, Sterner M, Stewart E, Thompson TT, Thornton J, Trujillo PJ, Volpe TJ, Enquist BJ (2012) The leaf-area shrinkage effect can bias paleoclimate and ecology research. *Am J Bot* 99: 1756-1763.
- Blonder B, De Carlo F, Moore J, Rivers M, Enquist BJ (2012) X-ray imaging of leaf venation networks. *New Phytol* 196: 1274-1282.
- Brodribb TJ, Feild TS, Jordan GJ (2007) Leaf maximum photosynthetic rate and venation are linked by hydraulics. *Plant Physiol* 144: 1890-1898.
- Brodribb TJ, Feild TS, Sack L. (2010) Viewing leaf structure and evolution from a hydraulic perspective. *Functional Plant Biol* 37: 488-498.
- Carminati A, Moradi AB, Vetterlein D, Vontobel P, Lehmann E, Weller U, Vogel H-J, Oswald SE (2010) Dynamics of soil water content in the rhizosphere. *Plant Soil* 332: 163-176.
- Cleveland TE, Hussey DS, Chen Z-Y, Jacobson DL, Brown RL, Carter-Wientjes C, Arif M (2008) The use of neutron tomography for the structural analysis of corn kernels. *J Cereal Sci* 48: 517-525.
- Defraeye T, Aregawi W, Saneinejad S, Vontobel P, Lehmann E, Carmeliet J, Verboven P, Derome D, Nicolai B (2013) Novel application of neutron radiography to forced convective drying of fruit tissue. *Food Bioproc Tech* 6: 3353-3367.

- Defraeye T., Derome D., Aregawi W., Cantré D., Hartmann S., Lehmann E., Carmeliet J., Voisard F., Verboven P., Nicolai B. (2014), Quantitative neutron imaging of water distribution, venation network and sap flow in leaves, *Planta* 240 (2), 423-436. <http://dx.doi.org/10.1007/s00425-014-2093-3>
- Dhondt S, Vanhaeren H, Van Loo D, Cnudde V, Inzé D (2010) Plant structure visualization by high-resolution X-ray computed tomography. *Trends Plant Sci* 15: 419-422.
- Dhondt S, Van Haerenborgh D, Van Cauwenbergh C, Merks RM, Philips W, Beemster GT, Inzé D (2012) Quantitative analysis of venation patterns of Arabidopsis leaves by supervised image analysis. *The Plant J* 69: 553-563.
- Esser HG, Carminati A, Vontobel P, Lehmann EH, Oswald SE (2010) Neutron radiography and tomography of water distribution in the root zone. *J Plant Nutr Soil Sc* 173: 757-764.
- Hassanein R, Lehmann E, Vontobel P (2005) Methods of scattering corrections for quantitative neutron radiography. *Nucl Instrum Meth A* 542: 353-360.
- Herremans E, Verboven P, Bongaers E, Estrade P, Verlinden B, Wevers M, Hertog M, Nicolai B (2013) Characterisation of 'Braeburn' browning disorder by means of X-ray micro-CT. *Postharvest Biol Tec* 75: 114-124.
- Ho QT, Verboven P, Verlinden BE, Herremans E, Wevers M, Carmeliet J, Nicolai BM (2011) A three-dimensional multiscale model for gas exchange in fruit. *Plant Physiol* 155: 1158-1168.
- Ho QT, Verboven P, Yin X, Struik PC, Nicolai BM (2012) A microscale model for combined CO<sub>2</sub> diffusion and photosynthesis in leaves. *PLoS ONE* 7: e48376.
- Jasechko S, Sharp ZD, Gibson JJ, Birks SJ, Yi Y, Fawcett PJ (2013) Terrestrial water fluxes dominated by transpiration. *Nature* 496: 347-350.
- Jeje AA (1985) The flow and dispersion of water in the vascular network of dicotyledonous leaves. *Biorheology* 22: 285-302.
- Kaestner AP, Hartmann S, Kühne G, Frei G, Grünzweig C, Josic L, Schmid F, Lehmann EH (2011a). The ICON beamline - A facility for cold neutron imaging at SINQ. *Nucl Instrum Meth A* 659: 387-393.
- Kaestner A, Münch B, Trtik P, Butler L (2011b) Spatiotemporal computed tomography of dynamic processes. *Opt Eng* 50: e123201.
- Kaiser H (2009) The relation between stomatal aperture and gas exchange under consideration of pore geometry and diffusional resistance in the mesophyll. *Plant Cell Environ* 32: 1091-1098.
- Kaufmann I, Schulze-Till T, Schneider HU, Zimmermann U, Jakob P, Wegner LH (2009) Functional repair of embolized vessels in maize roots after temporal drought stress, as demonstrated by magnetic resonance imaging. *New Phytol* 184: 245-256.
- Kawabata Y, Hino M, Matsushima U, Horie T, Nakano T, Maruyama R (2005) Cold and very cold neutron radiography for high contrast neutron imaging in Kyoto University Reactor. *J Radioanal Nucl Ch* 264: 319-324.

Defraeye T., Derome D., Aregawi W., Cantré D., Hartmann S., Lehmann E., Carmeliet J., Voisard F., Verboven P., Nicolai B. (2014), Quantitative neutron imaging of water distribution, venation network and sap flow in leaves, *Planta* 240 (2), 423-436. <http://dx.doi.org/10.1007/s00425-014-2093-3>

- Kim HK, Lee SJ (2010) Synchrotron X-ray imaging for non-destructive monitoring of sap flow dynamics through xylem vessel elements in rice leaves. *New Phytol* 188: 1085-1098.
- Kholova J, Hash CT, Kumar PL, Yadav RS, Kočová M, Vadez V (2010) Terminal drought-tolerant pearl millet [*Pennisetum glaucum* (L.) R. Br.] have high leaf ABA and limit transpiration at high vapour pressure deficit. *J Exp Bot* 61: 1431-1440.
- Kuroki S, Oshita S, Sotome I, Kawagoe Y, Seo Y (2004) Visualization of 3-D network of gas-filled intercellular spaces in cucumber fruit after harvest. *Postharvest Biol Tec* 33: 255-262.
- Lambers H, Chapin FS, Pons TL (2008) *Plant physiological ecology*. Springer Science + Business Media, New York.
- Lee SJ, Kim Y (2008) In vivo visualization of the water-refilling process in xylem vessels using X-ray micro-imaging. *Ann Bot-London* 101: 595-602.
- Marenco RA, Siebke K, Farquhar GD, Ball MC (2006) Hydraulically based stomatal oscillations and stomatal patchiness in *Gossypium hirsutum*. *Functional Plant Biol* 33 (12): 1103-1113.
- Matsushima U, Kawabata Y, Hino M, Geltenbort P, Nicolai B (2005a) Measurement of changes in water thickness in plant materials using very low-energy neutron radiography. *Nucl Instrum Meth A* 542: 76-80.
- Matsushima U, Kawabata Y, Horie T (2005b) Estimation of the volumetric water content in chrysanthemum tissues. *J Radioanal Nucl Ch* 264: 325-328.
- Matsushima U, Herppich WB, Kardjilov N, Graf W, Hilger A, Manke I (2009) Estimation of water flow velocity in small plants using cold neutron imaging with D<sub>2</sub>O tracer. *Nucl Instrum Meth A* 605: 146-149.
- Mendoza F, Verboven P, Mebatsion HK, Kerckhofs G, Wevers M, Nicolai B (2007) Three-dimensional pore space quantification of apple tissue using X-ray computed microtomography. *Planta* 226: 559-570.
- Moradi AB, Carminati A, Vetterlein D, Vontobel P, Lehmann E, Weller U, Hopmans JW, Vogel HJ, Oswald SE (2011) Three-dimensional visualization and quantification of water content in the rhizosphere. *New Phytol* 192: 653-663.
- Mott KA, Buckley TN (2000) Patchy stomatal conductance: emergent collective behaviour of stomata. *Trends Plant Sci* 5: 258-262.
- Nobel PS (2005) *Physicochemical and environmental plant physiology*. Elsevier Academic Press, London.
- Ogburn RM, Edwards EJ (2013) Repeated origin of three-dimensional leaf venation releases constraints on the evolution of succulence in plants. *Curr Biol* 22-23: 722-726.

- Defraeye T., Derome D., Aregawi W., Cantré D., Hartmann S., Lehmann E., Carmeliet J., Voisard F., Verboven P., Nicolai B. (2014), Quantitative neutron imaging of water distribution, venation network and sap flow in leaves, *Planta* 240 (2), 423-436. <http://dx.doi.org/10.1007/s00425-014-2093-3>
- Pérez-Harguindeguy N, Díaz S, Garnier E, Lavorel S, Poorter H, Jaureguiberry P, Bret-Harte MS, Cornwell WK, Craine JM, Gurvich DE, Urcelay C, Veneklaas EJ, Reich PB, Poorter L, Wright IJ, Ray P, Enrico L, Pausas JG, de Vos AC, Buchmann N, Funes G, Quétier F, Hodgson JG, Thompson K, Morgan HD, ter Steege H, van der Heijden MGA, Sack L, Blonder B, Poschlod P, Vaieretti MV, Conti G, Staver AC, Aquino S, Cornelissen JHC (2013) New handbook for standardised measurement of plant functional traits worldwide. *Aust J Bot* 61: 167–234.
- Rogiers SY, Greer DH, Hutton RJ, Landsberg JJ (2009) Does night-time transpiration contribute to anisohydric behaviour in a *Vitis vinifera* cultivar? *J Exp Bot* 60: 3751-3763.
- Rolland-Lagan AG, Amin M, Pakulska M (2009) Quantifying leaf venation patterns: two-dimensional maps. *The Plant J* 57: 195-205.
- Roth-Nebelsick A, Uhl D, Mosbrugger V, Kerp H (2001) Evolution and function of leaf venation architecture - a review. *Ann Bot-London* 87: 553-566.
- Sack L, Streeter CM, Holbrook NM (2004) Hydraulic analysis of water flow through leaves of sugar maple and red oak. *Plant Physiol* 134: 1824-1833.
- Sardans J, Penuelas J, Lope-Piedrafita S (2010) Changes in water content and distribution in *Quercus ilex* leaves during progressive drought assessed by in vivo  $^1\text{H}$  magnetic resonance imaging. *BMC Plant Biology* 10:188.
- Schuepp PH (1993) Tansley Review No. 59: Leaf boundary layers. *New Phytol* 125: 477-507.
- Scoffoni C, Vuong C, Diep S, Cochard H, Sack L (2013) Leaf shrinkage with dehydration: coordination with hydraulic vulnerability and drought tolerance. *Plant Physiol* 113: 221424.
- Sedighi-Gilani M, Griffa M, Mannes D, Lehmann E, Carmeliet J, Derome D (2012) Visualization and quantification of liquid water transport in softwood by means of neutron radiography. *Int J Heat Mass Tran* 55: 6211-6221.
- Van As H, Scheenen T, Vergeldt FJ (2009) MRI of intact plants. *Photosynth Res* 102: 213-222.
- Verboven P, Kerckhofs G, Mebatsion HK, Ho QT, Temst K, Wevers M, Cloetens P, Nicolai B (2008) 3-D gas exchange pathways in pome fruit characterised by synchrotron X-ray computed tomography. *Plant Physiol* 147: 518-527.
- Verboven P, Pedersen O, Herremans E, Ho QT, Nicolai B, Colmer TD, Teakle N (2012) Root aeration via aerenchymatous phellem: three dimensional micro-imaging and radial  $\text{O}_2$  profiles in *Melilotus siculus*. *New Phytol* 193: 420-431.
- Windt CW, Vergeldt FJ, de Jager PA, van As H (2006) MRI of long-distance water transport: a comparison of the phloem and xylem flow characteristics and dynamics in poplar, castor bean, tomato and tobacco. *Plant Cell Environ* 29: 1715-1729.

Defraeye T., Derome D., Aregawi W., Cantré D., Hartmann S., Lehmann E., Carmeliet J., Voisard F., Verboven P., Nicolai B. (2014), Quantitative neutron imaging of water distribution, venation network and sap flow in leaves, *Planta* 240 (2), 423-436. <http://dx.doi.org/10.1007/s00425-014-2093-3>

Wing SL (1992) High-resolution leaf X-radiography in systematics and paleobotany. *Am J Bot* 79: 1320-1324.

Zwieniecki MA, Melcher PJ, Boyce CK, Sack L, Holbrook NM (2002) Hydraulic architecture of leaf venation in *Laurus nobilis* L. *Plant Cell Environ* 25: 1445-1450.

## **FIGURE LEGENDS**

Fig. 1. Schematic overview of the experimental setup for cold neutron imaging in the ICON beamline (not to scale).

Fig. 2. Contours of distribution of effective water thickness ( $z_{w,eff}$ ), scaled with the surface-averaged water thickness ( $z_{w,eff,avg}$ ) for the five leaves scanned in the TOMO experiments (scaling ranges from 0.3 to 3.5). The high intensity region in the leaf lamina of tomato 1 is due to an overlap of the leaf tissue.

Fig. 3. Contours of distribution of effective water thickness ( $z_{w,eff}$ ), scaled with the surface-averaged water thickness ( $z_{w,eff,avg}$ ), i.e.  $z_{w,eff}/z_{w,eff,avg}$ , for the two leaves scanned in the RAD<sub>2</sub>O experiments (scaling ranges from 0.3 to 3.5). The initial images at the start of the experiment are shown, thus without D<sub>2</sub>O infiltration. The aluminium tape used to fix the leaves is visible in the radiograms (Fig. 3) as the glue on the tape also contained some hydrogen, resulting in some beam attenuation. The locations where aluminium tape was applied to fix the leaf are indicated with transparent grey regions, which have a larger apparent water thickness.

Fig. 4. Water content in cross sections of the leaf petioles for the five leaves scanned in the TOMO experiments, scaled with the maximal water content in each individual section ( $w/w_{max}$ , scaling ranges from 0.1 to 1).

Fig. 5. Water content in cross sections of the leaf (left image for each leaf), scaled with the maximal water content in each individual section (scaling ranges from 0.1 to 1), i.e.  $w/w_{max}$ ; and contours of distribution of effective water thickness ( $z_{w,eff}$ ) (right image for each leaf), scaled with the surface-averaged water thickness ( $z_{w,eff,avg}$ ) (scaling ranges from 0.3 to 3.5) for two leaves scanned in the TOMO experiments, i.e.  $z_{w,eff}/z_{w,eff,avg}$ .

Defraeye T., Derome D., Aregawi W., Cantré D., Hartmann S., Lehmann E., Carmeliet J., Voisard F., Verboven P., Nicolai B. (2014), Quantitative neutron imaging of water distribution, venation network and sap flow in leaves, *Planta* 240 (2), 423-436. <http://dx.doi.org/10.1007/s00425-014-2093-3>

Fig. 6. Contours of change of water thickness  $\Delta z_w$  over time (absolute value, i.e., positive), scaled with the surface-averaged water thickness at the start of the experiment ( $z_{w,eff,avg}$ ), during D<sub>2</sub>O uptake for the two leaves scanned in the RAD<sub>2</sub>O experiments (scaling ranges from 0.3 to 3.5), i.e.  $\Delta z_w/z_{w,eff,avg}$ . The contours are given for every hour after the start of the experiment.

Fig. 7. Water loss ( $\Delta m_{w,tot}$ , absolute value, i.e., positive) for the two leaves scanned in the RAD<sub>2</sub>O experiments over time.

Supplemental Fig. S1. Experimental setups for neutron tomography ((a) TOMO) and radiography of D<sub>2</sub>O uptake ((b) RAD<sub>2</sub>O) with indication of main parts (alu.: aluminium) and dimensions (in mm, not to scale).

Supplemental Fig. S2: Tomograms of a tomato and an apple leaf, where the first and second order venation architecture is indicated in brown (third order venation was difficult to segment from the tomograms).

## **TABLES**

Table 1. Mass of water in leaves from gravimetric measurements and neutron imaging (with and without scattering correction) together with leaf surface area, mass of the leaf dry matter and the average initial leaf water thickness for the TOMO experiments.

Sample	Gravimetric			Neutron imaging					
	Area (cm <sup>2</sup> )	Water mass (mg)	Mass leaf dry matter (%)	Water thickness (µm)	Water mass (mg)	Difference	Water mass (mg)	Difference	Scattering vs. no scattering Difference
	$A_f$	$m_{w,0}$	$m_d/m_{w,0}$	$z_{w,0,avg}$	$m_{w,eff,tot}$	$\frac{m_{w,eff,tot} - m_{w,0}}{m_{w,0}}$	$m_{w,eff,tot,ns}$	$\frac{m_{w,eff,tot,ns} - m_{w,0}}{m_{w,0}}$	$\frac{m_{w,eff,tot} - m_{w,eff,tot,ns}}{m_{w,eff,tot}}$
Tomato 1	10.7	216	13%	201	232	7%	218	1%	6%
Tomato 2	10.1	230	12%	227	244	6%	232	1%	5%
Tomato 3	12.2	277	11%	226	292	6%	271	-2%	7%
Apple 1	8.9	127	33%	143	160	26%	152	20%	5%
Apple 2	11.4	166	36%	146	220	33%	205	24%	7%

Defraeye T., Derome D., Aregawi W., Cantré D., Hartmann S., Lehmann E., Carmeliet J., Voisard F., Verboven P., Nicolai B. (2014), Quantitative neutron imaging of water distribution, venation network and sap flow in leaves, *Planta* 240 (2), 423-436. <http://dx.doi.org/10.1007/s00425-014-2093-3>

Table 2. Initial mass of water in leaves from neutron imaging (with scattering correction) together with leaf surface area and the average initial leaf water thickness for the RAD<sub>2</sub>O experiments.

Sample	Neutron imaging		
	Area (cm <sup>2</sup> )	Water mass (mg)	Water thickness (μm)
	$A_f$	$m_{w,eff,tot}$	$z_{w,eff,avg}$
Tomato	3.4	48	140
Apple	2.9	28	95

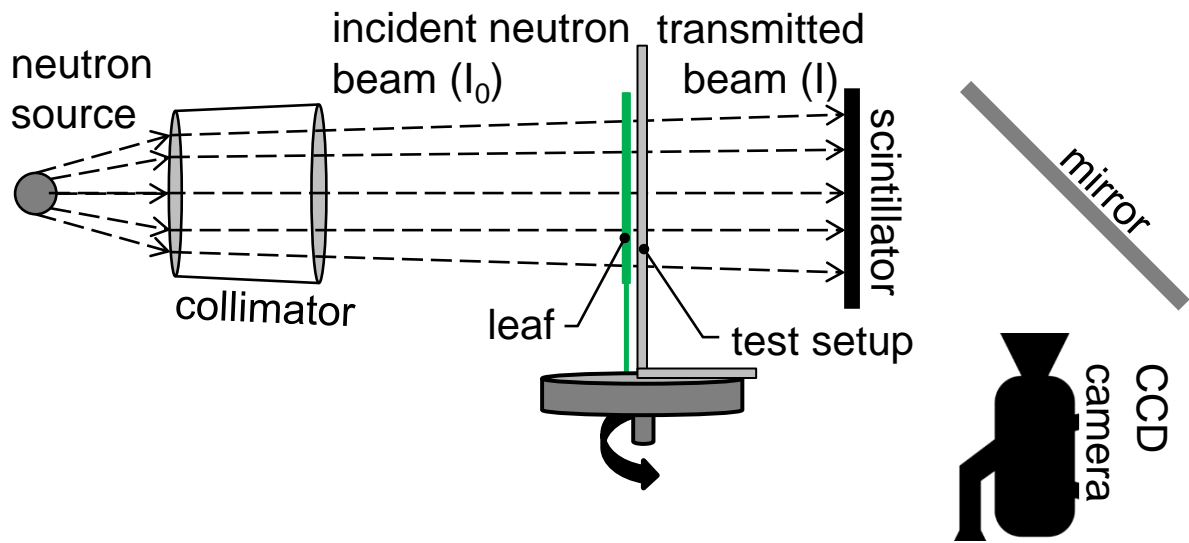


Figure 1. Schematic overview of the experimental setup for cold neutron imaging in the ICON beamline (not to scale).

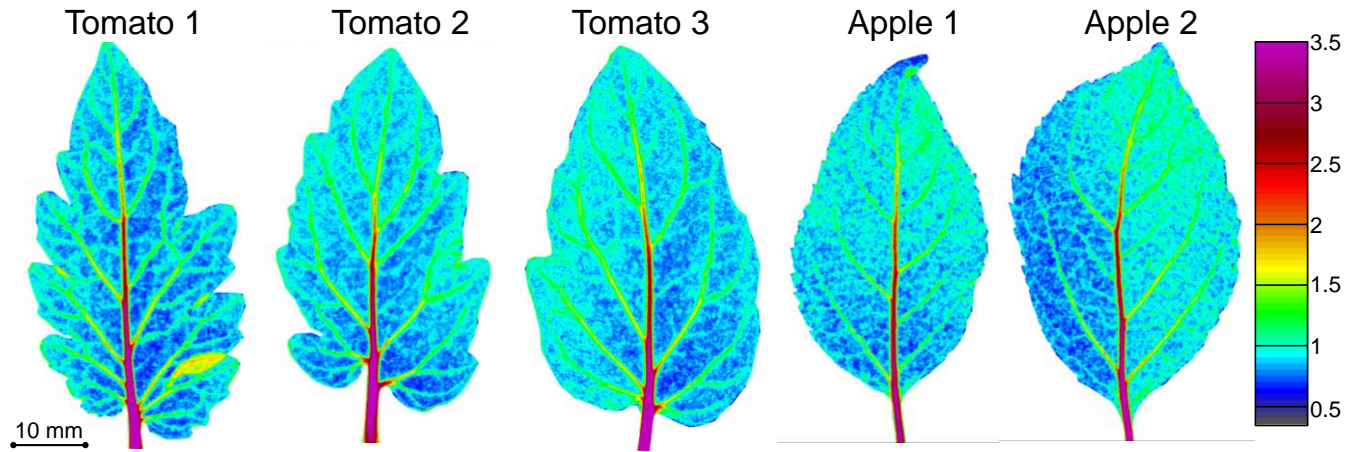


Figure 2. Contours of distribution of effective water thickness ( $z_{w,eff}$ ), scaled with the surface-averaged water thickness ( $z_{w,eff,avg}$ ) for the five leaves scanned in the TOMO experiments (scaling ranges from 0.3 to 3.5). The high intensity region in the leaf lamina of tomato 1 is due to an overlap of the leaf tissue.

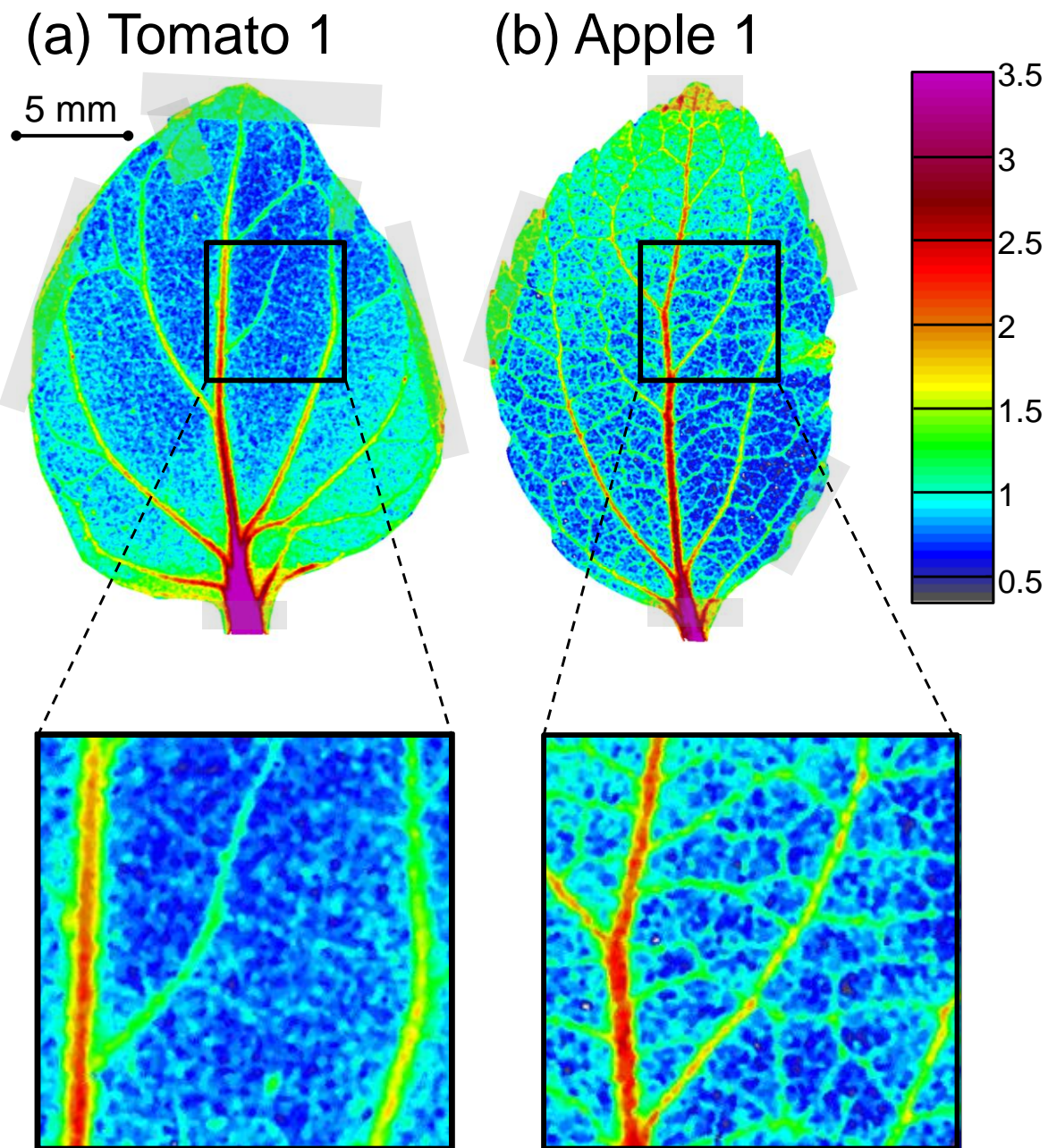


Fig. 3. Contours of distribution of effective water thickness ( $z_{w,eff}$ ), scaled with the surface-averaged water thickness ( $z_{w,eff,avg}$ ), i.e.  $z_{w,eff}/z_{w,eff,avg}$ , for the two leaves scanned in the RAD<sub>2</sub>O experiments (scaling ranges from 0.3 to 3.5). The initial images at the start of the experiment are shown, thus without D<sub>2</sub>O infiltration. The aluminium tape used to fix the leaves is visible in the radiograms (Fig. 3) as the glue on the tape also contained some hydrogen, resulting in some beam attenuation. The locations where aluminium tape was applied to fix the leaf are indicated with transparent grey regions, which have a larger apparent water thickness.

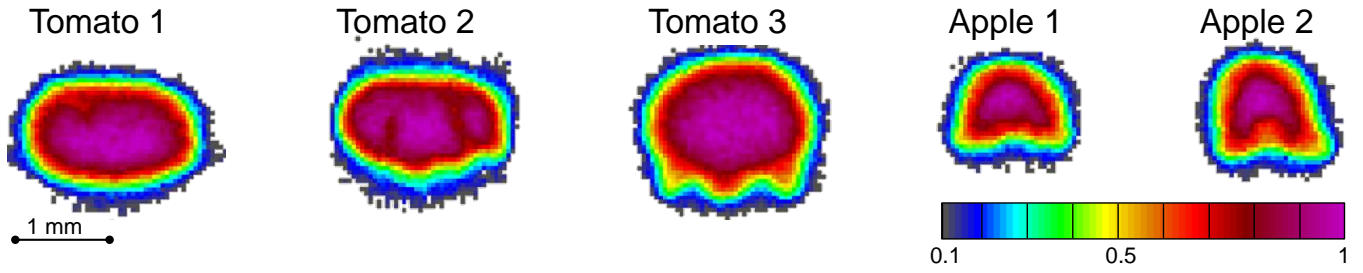


Fig. 4. Water content in cross sections of the leaf petioles for the five leaves scanned in the TOMO experiments, scaled with the maximal water content in each individual section ( $w/w_{max}$ , scaling ranges from 0.1 to 1).

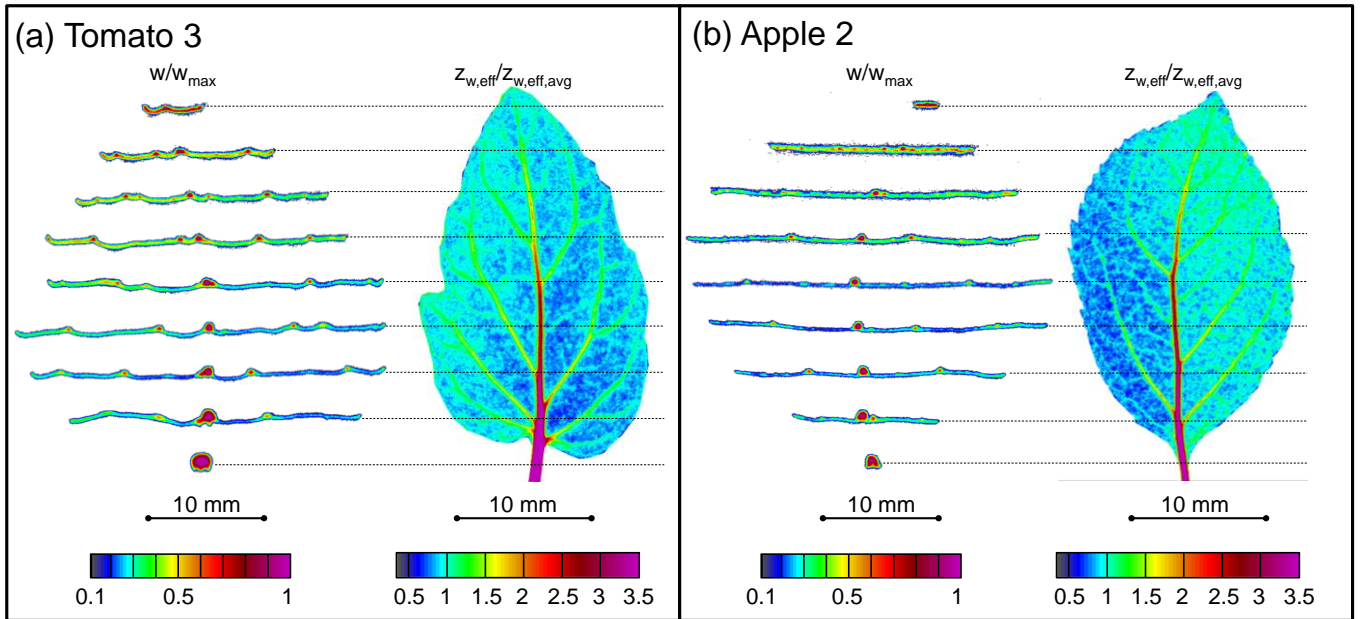


Fig. 5. Water content in cross sections of the leaf (left image for each leaf), scaled with the maximal water content in each individual section (scaling ranges from 0.1 to 1), i.e.  $w/w_{max}$ ; and contours of distribution of effective water thickness ( $z_{w,eff}$ ) (right image for each leaf), scaled with the surface-averaged water thickness ( $z_{w,eff,avg}$ ) (scaling ranges from 0.3 to 3.5) for two leaves scanned in the TOMO experiments, i.e.  $z_{w,eff}/z_{w,eff,avg}$ .

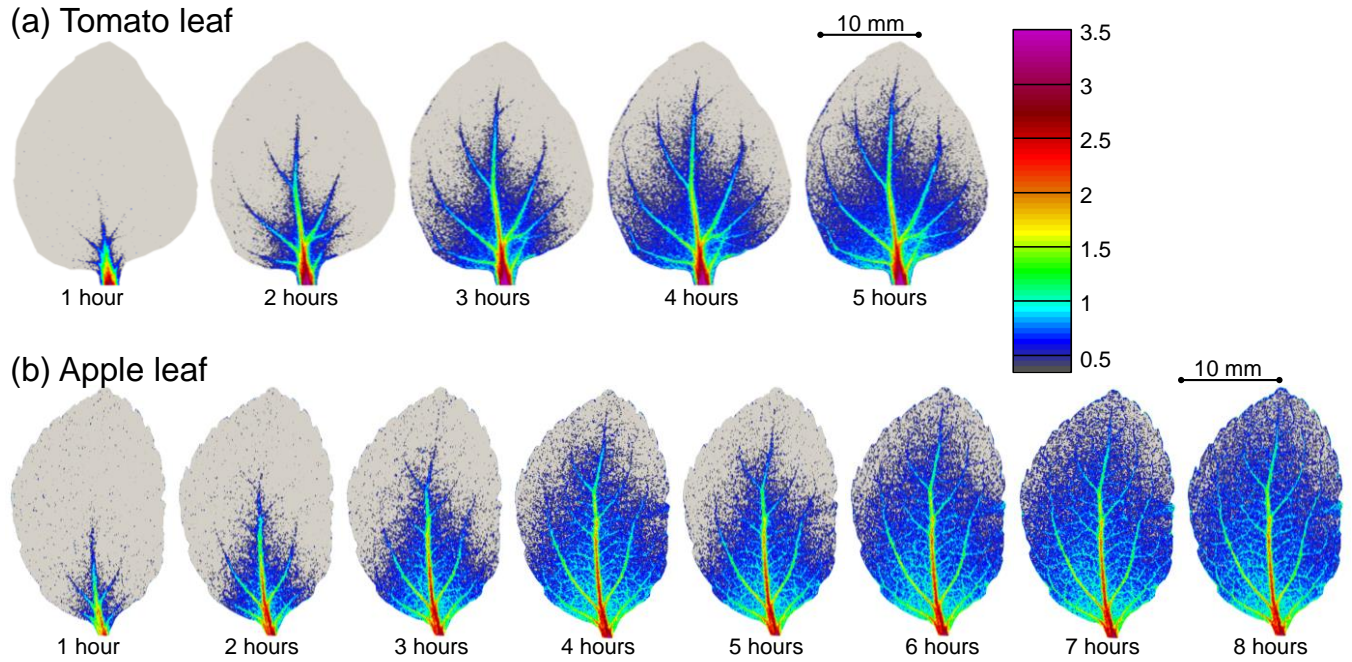


Fig. 6. Contours of change of water thickness  $\Delta z_w$  over time (absolute value, i.e., positive), scaled with the surface-averaged water thickness at the start of the experiment ( $z_{w,eff,avg}$ ), during  $D_2O$  uptake for the two leaves scanned in the  $RAD_2O$  experiments (scaling ranges from 0.3 to 3.5), i.e.  $\Delta z_w/z_{w,eff,avg}$ . The contours are given for every hour after the start of the experiment.

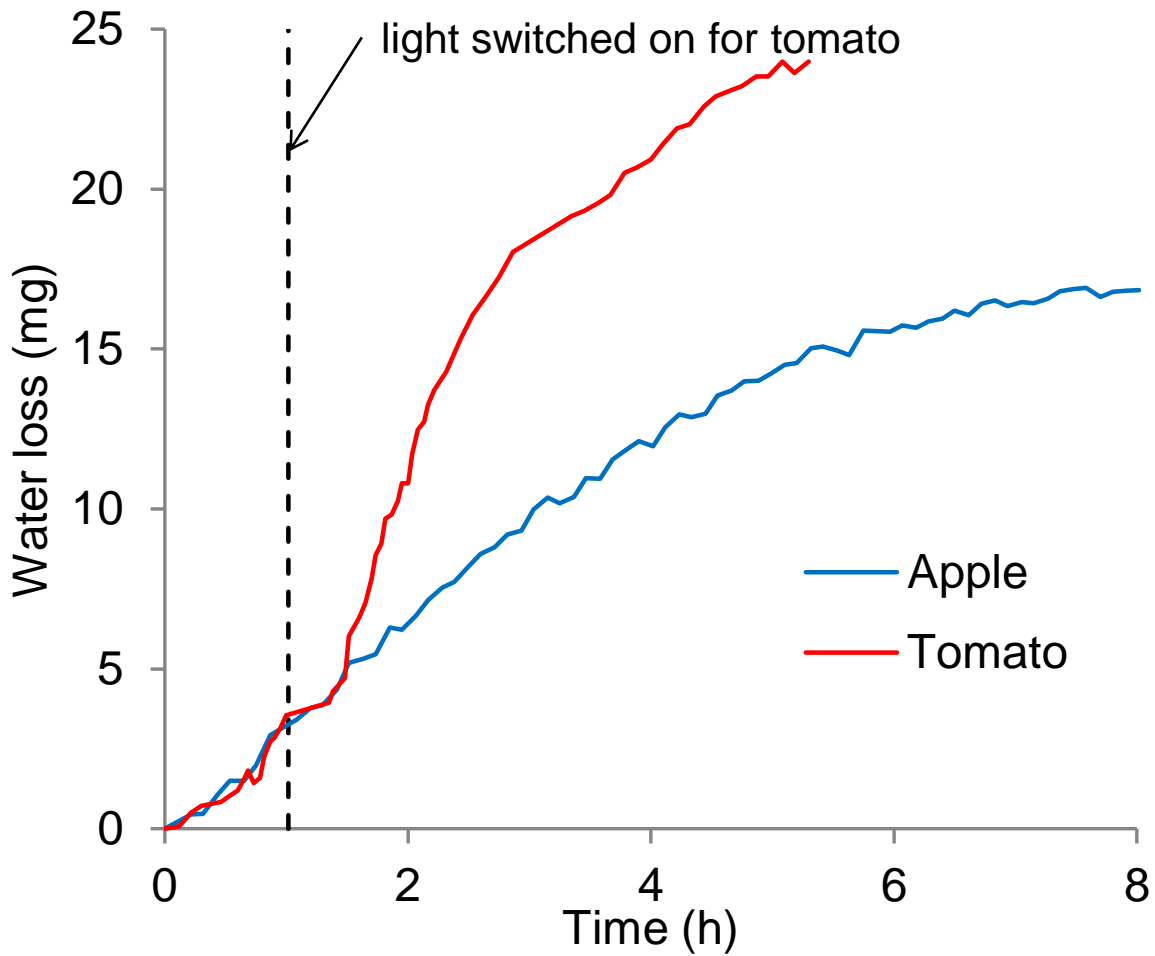


Figure 7. Water loss ( $\Delta m_{w,tot}$ , absolute value, i.e., positive) for the two leaves scanned in the RAD<sub>2</sub>O experiments over time.

## **Supplementary Data**

### **Notes S1: Calculation of reduction in water thickness**

The D<sub>2</sub>O uptake and water loss caused a reduction of the effective water thickness ( $z_{w,eff}$ ) over time ( $t$ ). Here, the reduction in water thickness was determined. Eq. (2) is rewritten as:

$$I(t) = I_0 e^{-(\Sigma_{LT} z_{LT} + \Sigma_{TS} z_{TS} + \Sigma_w z_w(t) + \Sigma_{D2O} z_{D2O}(t))} = I_0 e^{-(\Sigma_{LT} z_{LT} + \Sigma_{TS} z_{TS} + \Sigma_w (z_w(t_0) + \Delta z_w(t)) + \Sigma_{D2O} (z_{D2O}(t_0) + \Delta z_{D2O}(t)))} \quad (S1)$$

where  $t_0$  is the time of the first neutron radiogram at the start of the uptake experiment,  $z_w(t_0)$  is the initial water thickness,  $z_{D2O}(t_0)$  is the initial D<sub>2</sub>O thickness which is equal to zero,  $\Delta z_w(t)$  is the reduction in water thickness at time  $t$  due to water loss from the leaf during D<sub>2</sub>O uptake (transpiration and outflow), which has a negative value, and  $\Delta z_{D2O}(t)$  is the corresponding increase of D<sub>2</sub>O thickness, which has a positive value. Since the change in neutron beam attenuation with time was entirely caused by the change of water and D<sub>2</sub>O content in the sample, these relative changes ( $\Delta z_w(t)$  and  $\Delta z_{D2O}(t)$ ) could be determined by relating all radiograms to the first radiogram, by rewriting Eq. (S1):

$$I(t) = I(t_0) e^{-(\Sigma_w \Delta z_w(t) + \Sigma_{D2O} \Delta z_{D2O}(t))} \quad (S2)$$

$$\text{with } I(t_0) = I_0 e^{-(\Sigma_{LT} z_{LT} + \Sigma_{TS} z_{TS} + \Sigma_w z_w(t_0) + \Sigma_{D2O} z_{D2O}(t_0))} \quad (S3)$$

where  $I(t_0)$  is the intensity of the neutron beam for the initial, freshly-cut leaf sample, i.e., at the start of the neutron experiments.  $I(t_0)$  was lower than  $I(t)$  (exponent to  $-(\Sigma_w \Delta z_w(t) + \Sigma_{D2O} \Delta z_{D2O}(t)) > 1$ ) since the amount of water in the sample decreased due to water transpiration and outflow, and was replaced by D<sub>2</sub>O, which attenuates much less than water:  $\Sigma_{D2O} = 0.5 \text{ cm}^{-1}$  (for the present study) is much smaller than  $\Sigma_w = 5.13 \text{ cm}^{-1}$ . As such, the change in beam attenuation was predominantly due to a decrease of water content, rather than an increase of D<sub>2</sub>O. If assuming that  $\Delta z_{D2O}$  can be approximated by  $-\Delta z_w$ , i.e., the amount of water lost is entirely replaced by D<sub>2</sub>O, Eq. (S2) can be solved to the change in water thickness ( $\Delta z_w(t) < 0$ ):

$$\Delta z_w(t) = -\frac{1}{(\Sigma_w - \Sigma_{D2O})} \left[ \ln \left( \frac{I(t)}{I(t_0)} \right) \right] \quad (S4)$$

## **Notes S2: Image corrections for neutron radiograms**

Following corrections were made for the raw neutron radiograms, using standard procedures common to all radiation transmission-based imaging methods, together with a scattering correction as required for neutron radiography:

1. *Dark current correction* for the background noise of the CCD camera, performed by subtracting (pixelwise) the radiogram acquired in absence of a neutron beam from each radiogram of the sample.
2. *Intensity correction* for fluctuations of the incident beam, performed by averaging the beam variation in an area of the radiogram outside the sample area and applying this averaged correction factor to each pixel.
3. *Flat field correction* for eliminating spatial inhomogenities in the beam (and detector) from the radiograms, performed by correcting (pixelwise) each radiogram with a radiogram with an open beam, without the setup.
4. *Black body correction* for removing the neutron signal coming from scattering by the overall experimental configuration and environment, performed by subtracting a constant value from each radiogram of the sample. For this constant value, the average value of the beam variation in the sample area is taken for a radiogram acquired when the sample is shielded with boronated polyethylene blocks.
5. *Sample scattering correction* for neutrons that are scattered at small angles by the atoms of the leaf tissue, water or test setup. Due to lack of information on the scattering properties of the leaf tissue, the scattering correction was performed assuming water as the only scattering material.
6. *Taking into account the beam polychromatic energy spectrum*, as the aforementioned equations are derived for a monochromatic neutron beam.

To perform these corrections, the Quantitative Neutron Imaging (QNI) algorithm, developed by Hassanein (2006), was used, with adjusted parameters for imaging with cold neutrons. Especially the scattering correction is advised for increased accuracy. The QNI scattering correction algorithm is based on the iterative reconstruction of the measured image by overlapping point scattered functions calculated by means of Monte-Carlo simulation. By means of the QNI correction, Hassanein *et al.* (2005) found errors in water thickness below 5% for water thicknesses from 1 mm up to 5 mm for thermal neutrons. In the present study, the water thickness of the samples was quite low (~ 100-200  $\mu\text{m}$ , see section 3.1), resulting in limited attenuation of the neutron beam and thus relatively little scattering, by which a scattering correction is perhaps not required. The impact of the scattering correction for leaves was evaluated in section 3.1. From QNI, the water (mass)

Defraeye T., Derome D., Aregawi W., Cantré D., Hartmann S., Lehmann E., Carmeliet J., Voisard F., Verboven P., Nicolai B. (2014), Quantitative neutron imaging of water distribution, venation network and sap flow in leaves, *Planta* 240 (2), 423-436. <http://dx.doi.org/10.1007/s00425-014-2093-3>

thickness ( $z_w$  or  $Z_w$ ) was estimated as a single variable and was used for subsequent quantitative analysis (as described in sections 2.4.1 and 2.4.2).

The resolution in water thickness ( $R$ , dynamic range) is defined as the water thickness corresponding to one greyscale level difference with the incident neutron beam intensity (see Eq. (1)):

$$R = -\frac{1}{\Sigma_w} \ln\left(\frac{I_0 - 1}{I_0}\right) \quad (\text{S5})$$

A water thickness resolution of 0.1  $\mu\text{m}$  (TOMO) and 0.14  $\mu\text{m}$  (RAD<sub>2</sub>O) was obtained, which resulted in a dynamic range of roughly about 2000 (TOMO) or 700 (RAD<sub>2</sub>O) greyscale levels detectable over a leaf, assuming a leaf water thickness of 200  $\mu\text{m}$  (TOMO) and 100  $\mu\text{m}$  (RAD<sub>2</sub>O).

**Figure S1: Experimental setups for neutron imaging.**

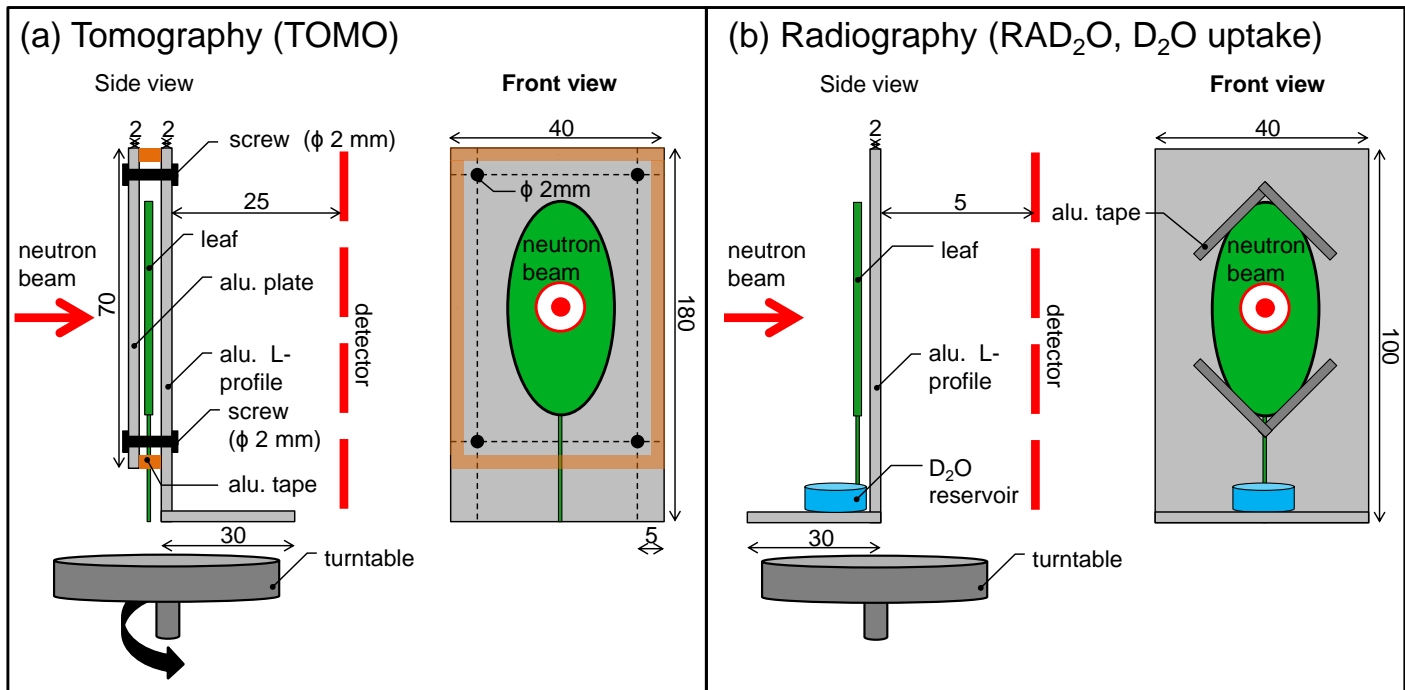


Figure S1. Experimental setups for neutron tomography ((a) TOMO) and radiography of D<sub>2</sub>O uptake ((b) RAD<sub>2</sub>O) with indication of main parts (alu.: aluminium) and dimensions (in mm, not to scale).

**Figure S2: Tomograms of a tomato and an apple leaf.**

(a) Tomato 1



(b) Apple 1



Figure S2. Tomograms of a tomato and an apple leaf, where the first and second order venation architecture is indicated in brown (third order venation was difficult to segment from the tomograms).